IMPACT OF FAULT AND CABLE CHARACTERISTICS ON FAULT LOCATION ACCURACY OF UNDERGROUND CABLES

by

Aryan Hoorjandi

A thesis submitted to the faculty of
The University of North Carolina at Charlotte
in partial fulfillment of the requirements
for the degree of Master of Science in
Electrical Engineering

Charlotte

2026

Approved by:

_____
Dr. Valentina Cecchi

_____
Dr. Arun Shrestha

_____
Dr. Badrul Chowdhury

ABSTRACT

ARYAN HOORJANDI. Impact Of Fault and Cable Characteristics on Fault Location Accuracy of Underground Cables. (Under the direction of DR. VALENTINA CECCHI and DR. ARUN SHRESTHA)

With the rise in the use of underground cables across different electric grids, the need for accurate and dependable fault location identification of underground transmission and distribution systems is paramount to ensuring that the advantages of Underground (UG) lines are maintained. Notable advantages offered by UG cables include increased resilience and reliability against adverse events, improved public safety in cases of accidents, and arc-flash-induced wildfire mitigation. However, they are accompanied by a set of challenges in their modeling, protection, and fault location estimation, stemming from their special electrical characteristics. Namely, higher shunt capacitances, lower series inductances, large charging currents, and non-linear zero sequence impedances.

The most reliable fault locating methods include the double-ended traveling-wave (DE-TW) and the double-ended impedance-based (DE-Z) method. The DE-TW method requires the first TW arrival time to the two local and remote terminals. The DE-Z method uses metered voltages and current from both terminals to perform its fault location calculations. Both methods utilize two relays at different ends of the protected line to communicate through a direct fiber-optic channel or a C37.94 encoding digital channel.

Based on filed data, the general convention is that impedance-based fault location is accurate for overhead transmission lines and short underground cables. However, due to the complex electrical behavior of UG cables, especially the nonlinear zero-sequence impedance, accuracy of the DE-Z method becomes more limited in long underground lines. Traveling-wave

fault location is much more immune to the hard-to-predict characteristics of UG cables due to its high frequency wave detection, so long as the cable's propagation velocity is correctly calculated, which is used in the fault locating calculations. The DE-TW method's robustness aids in detecting more accurate fault locations, especially in long underground cables and hybrid lines consisting of overhead and underground sections.

The aim of this research is to set up a hardware-in-the-loop (HIL) test to study the extent to which different fault and XLPE cable characteristics affect the accuracy of the DE-TW and DE-Z fault locating methods. These fault characteristics include the fault type, fault location, fault resistance, and fault inception angle (fault-point-on-wave). The cable characteristics include cable core transposition and bonding/grounding of the cable sheath.

ACKNOWLEDGEMENTS

First, I would like to sincerely thank my advisors, Dr. Valentina Cecchi from the Electrical & Computer Engineering department at UNC Charlotte and Dr. Arun Shrestha from Schweitzer Engineering Laboratories, whose continued support, dedication, and expertise guided me through the master's program.

Lessons from Dr. Cecchi's power engineering courses and her tireless mentorship throughout my academic career have been invaluable for my understanding of many electrical engineering concepts and research methodologies. Her commitment to meeting advising me on all subjects truly helped me stay on track and gain the confidence I needed to accomplish this task.

I was very fortunate to be mentored by and work with Dr. Shrestha, whose vast technical expertise in power system modeling and with SEL devices was instrumental in giving me the knowledgebase to set up and conduct my research. His passion for research and knowledge inspired and enabled me to learn from real-world experiences and apply them to my research.

I would also like to greatly appreciate Professor Badrul Chawdhury for his insightful courses in power engineering which gave me a strong foundation of the concepts used in the electrical engineering filed, as well as his prudent feedback as a member of my committee.

I would like to send my sincere gratitude to Schwitzer Engineering Laboratories, which provided me with all the specialized equipment I needed to carry out my research and gave me the opportunity to work and learn while completing my degree. I am also grateful for the PATH program which provided financial support in this endeavor.

I am immeasurably indebted to my family and friends who supported me through all the tough times and gave me the love and inspiration that aided me in achieving all that I have. Thank you for all the patience and dedication that you showed throughout the years.

DEDICATION

This thesis is dedicated to my dear parents, Parisa Molavi and Reza Hoorjandi, whose unconditional love, unrelenting support, and immense sacrifices have given me the opportunity to pursue my goals and dreams.

TABLE OF CONTENTS

LIST OF TABLES

LIST OF FIGURES

LIST OF ABBREVIATIONS

UG	Underground
TW	Traveling-Wave
TWLPT	Traveling Wave Line Propagation Time
FL	Fault Location
DE	Double-Ended
DE-TW	Double-Ended Traveling-Wave
DE-Z	Double-Ended Impedance-Based
Z0	Zero-Sequence Impedance
Z1	Positive-Sequence Impedance
Z2	Negative-Sequence Impedance
I0	Zero-Sequence Current
I1	Positive-Sequence Current
I2	Negative-Sequence Current
DCB	Directional Comparison Blocking
POTT	Permissive Overreaching Transfer Trip
HIL	Hardware-in-the-loop
COMTRADE	Common Format for Transient Data Exchange
POW	Point-on-Wave
TOW	Top-of-Waveform
MOW	Middle-of-Waveform
ZC	Zero-Crossing
Ph-Gnd	Single Phase to Ground

2-Ph-Gnd	Double Phase to Ground
Ph-Ph	Phase to Phase
3Ph	Three Phase

CHAPTER 1: INTRODUCTION

1.1 Overview

Modeling and studying underground (UG) cables presents challenges caused by the unique electrical characteristics of UG cables, especially under different fault conditions. The zero-sequence impedance of UG cables can have a nonlinear behavior. This nonlinearity is due to a number of factors, namely, magnetic saturation, sheath bonding, and the fault current return path(s). UG cables also have greater shunt capacitances as a result of their much closer proximity to the ground compared to overhead lines, as well as the cable sheath, insulation dielectric constant, and the existence of different metallic structures in the vicinity of where the cable is laid out [1].

Protection and fault location (FL) identification of underground cables face many of the same challenges that cable modeling does. The notable contributors to the complexity and difficulty of UG cable protection include higher shunt capacitance, lower series inductance, variable zero-sequence impedance, and large charging currents. Given these additional intricacies of UG cables, conventional protection philosophies employ a primary protection element, commonly Line Current Differential (87L), and backup protection such as Directional Comparison (POTT/DCB) or Distance Protection [2].

Locating faults along underground cables is primarily done using two methods: Double-Ended Traveling-Wave (DE-TW) fault location, and Double-Ended Impedance-Based (DE-Z) fault location. The DE-TW FL method is the most reliable based on proven field data. It offers immunity against some of the idiosyncrasies of UG cables such as the large charging currents [2]. So long as the TW specific settings are configured accurately, fault location using this technique should yield reasonably accurate results. Impedance-

based FL can be prone to errors in UG cables resulting from the cable's nonlinear Z0, large shunt capacitances affecting the impedance profile, and high charging currents [2].

The presence of new variables and complexities in UG cables, coupled with the fact that they have been less commissioned and studied compared to overhead lines, leads to greater uncertainty when it comes to working with cables. However, the existing research and field data give a very helpful insight into how the complexities can be simplified so as to make the application of existing modeling, protection, and fault location principles more feasible for hybrid lines (mixed overhead and underground).

The intent of this research is to assess the effects of different fault and cable characteristics on the accuracy of the two FL methods. For this, a series of tests were designed with different sets of fault conditions and cable arrangements to examine their respective impacts on the accuracy of each FL method and determine practical findings to be used by engineers designing protection and monitoring systems for the power grid.

1.2 Underground Cables in Power Systems

Underground cables offer a myriad of advantages, such as enhanced reliability, increased public safety, mitigated wildfire risks, reduced electromagnetic emissions and losses, as well as improved aesthetics [3]. However, they introduce a new set of challenges that need to be accounted for in order to utilize the benefits. These include, much higher installation costs, limitations in power transfer capacity, restrictions in length and/or voltage levels, difficulties in fault detection and repair [3].

Global events such as climate-change-induced natural disasters and international conflicts have demonstrated a need for the additional reliability and security that underground cables offer. Coupled with the public's interest in the improved visuals and

the added safety of UG cables, more utility companies are using underground cables as major parts of their transmission and distribution networks. Therefore, the drive for incorporating UG cables into the existing power systems has created a need for the development of new techniques and technologies to accommodate the operation, protection, and maintenance needs of UG cables.

In operations for instance, shunt reactors are used for reactive power compensation to control the voltage levels in mitigating the Ferranti effect [4] and to provide some of the high charging current caused by the much higher capacitance of UG cables [5]. This allows for UG cable lines with much longer lengths and higher operating voltages which can also handle greater loads.

Protection of UG cables also has its share of challenges that need to be addressed. These challenges stem from the increased shunt capacitance of buried cables, nonlinearity of Z0 due to the variability of ground return paths, and the high charging currents caused by the large capacitance. In order to mitigate these issues, a primary and secondary set of protection systems are used with many considerations for the electrical characteristics of UG cables in setting the protections elements and schemes [1].

Given that UG cables are for the most part buried and there is limited access to the cables in select locations through utility holes, accurately locating faults is ever more valuable. The importance of accurate fault location detection in UG cables is amplified by the fact that their repair can take much longer than traditional overhead lines since they need to be dug up and are more complex to repair and replace. Therefore, a reliable fault locating mechanism is very helpful to operators and line-workers, who rely on accurate

location detection to reenergize the faulted sections as soon as possible. For this, the two most reliable methods are the DE-TW and the DW-Z FL method [2].

1.3 Underground Cables

1.3.1 Common Underground Cable Types

There are three types of underground cables that are most commonly used, High-Pressure Pipe-Type Cables, Self-Contained Fluid-Filled (SCFF) Cables, and Solid Dielectric Cross-Linked Polyethylene (XLPE) cables [1]. Each of these types has their own set of electrical characteristics, advantages, and disadvantages. For the purposes of this paper, Solid Dielectric cables will be used given their widespread use across the industry because of the greater benefits they offer as will be discussed.

1.3.1.1 Pipe-Type High-Pressure Fluid-Filled (HPFF)

The Pipe-Type High-Pressure Fluid-Filled (HPFF) and Gas-Filled (HPGF) cables have very similar design, construction, and configuration. They commonly use copper or aluminum conductors and paper tape or polypropylene paper laminate insulation inside spiral shield wire drenched in hydrocarbon fluid in HPFFs and Nitrogen gas in HPGFs. These cables are usually laid in 3-phase trefoil formation with metal shielding (lead) and skid wires inside steel pipes with an operational voltage range of 200-345 kV for HPFFs and 100-150 kV in HPGFs. Even though the pipe systems are tough, there are concerns with fluid leakage from HPFFs which pose serious environmental concerns. Leakage of HPGFs is less concerning. However, they have lower capacities given that the pressurized gas is a less effective insulator. The steel pipe acts as the sheath which is continuously grounded. The ground fault current magnitude affects the zero-sequence impedance which leads to a nonlinear Z0. The relationship between the current in each phase and the voltage

drop along these cables is also nonlinear as a result of the nonlinear magnetic characteristic of the coupling between the conductors and the steel pipe [1].

1.3.1.2 Self-Contained Fluid Filled (SCFF) Cables

Self-Contained Fluid Filled (SCFF) cables are internally pressurized with a dielectric fluid at 5-15 psi in old systems and 25-75 psi in new systems. Each phase is independently housed in a hermetically sealed metallic sheath made of extruded aluminum or lead with insulation tape. The hollow core of the conductors is used to maintain fluid pressure. The seamless design of the metallic sheath creates a uniform and strong seal to maintain pressure and stop moisture penetration, which is why these cable types are commonly used for underwater transmission. The Zero-sequence impedance depends mainly on the sheath bonding and the resistivity of the earth surrounding the cable. The bonding scheme of these cables greatly affects the circulating current and the zero-sequence impedance [1].

1.3.1.3 Solid Dielectric Cross-Linked Polyethylene (XLPE) Cables

Solid Dielectric cables have a single copper or aluminum core with cross-linked polyethylene (XLPE) insulation and a metallic screen or sheath. The three phases are usually installed in a trefoil formation and either directly buried, ducted, or tunnel-installed. They have a smaller capacitance and thus a lower steady-state charging current as well as lower losses, both of which increase their capacity for supporting greater loads. XLPE cables operate at voltages of up to 500 kV, high-voltage (HV) and Extra High Voltage (EHV), and their dimensions directly correlate with the cable's voltage levels. Unlike other cable types which need time for re-pressurization, XLPE cable can be reenergized

immediately after a fault if there is no permanent damage to the cable [1]. A diagram of an XLPE cable can be seen in Figure 1.1 showing the different layers [1]:

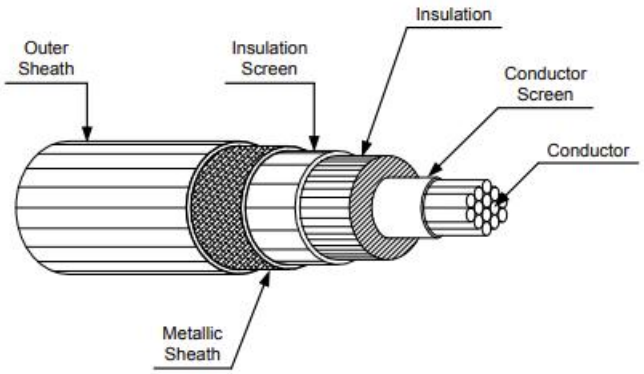

Figure 1.1 Layers of an XLPE Cable [1]

1.3.2 Underground Cable Characteristics

Electrical characteristics of high-voltage underground cables are quite different from overhead lines and can pose additional difficulties in modeling and short-circuit calculations because of the nonlinear behavior and complexities they introduce. Due to the conductors being much closer to the ground and the existence of the grounded sheath, plus the insulation material which has a relative permittivity that is much higher than that of air, the shunt capacitance across the cable can be 30-40 times higher than overhead transmission lines [1]. Since underground cables are typically laid out in a trefoil formation, the closeness of the conductors to one another leads to a series inductance that is 30-50% lower than overhead lines [1].

The reliability of any protection element which uses the zero-sequence impedance can be compromised due to the highly variable zero-sequence impedance that depends on the sheath bonding and ground return paths, which can be the cable sheath, ground, sheath and ground in parallel, or any water/gas pipes, railroad, or adjacent cables. The nonlinear Z0 and the location-dependency of the fault make distance protection unreliable [1].

The higher capacitance leads to much larger charging currents (even with no loads), which affects the reliability of distance elements (due to the apparent impedance shift), directional elements (especially $3I_2$, $3I_0$), differential protection (unbalanced capacitor current following into the 87L zone, and CT saturation risks) [5]. The high charging currents also create limitations for the minimum fault current settings as the large current magnitudes can falsely be detected as faults [1]. For instance, as shown in the SCE paper in a 500 kV system with a total of 70 miles of overhead and 4 miles of XLPE underground cable, the cable draws approximately 20 times as much charging current as an overhead line [2]. Based on the formula for calculating the charging current shown below:

$$I_{chrg} = \frac{j\omega C_1 V_{pp}}{\sqrt{3}} \tag{1.1}$$

The charging current is directly related to the positive sequence capacitance of the line. Therefore, a twenty-fold increase in the chagrin current for a 500 kV system matches expectations [2].

1.4 Underground Cable Protection Review

Faults on HV UG cables can have significantly different characteristics than those on overhead lines. When designing protection schemes and setting protection elements, engineers need to account for such factors as the high charging currents, the larger shunt capacitance of the line, the multitude of ground current return paths impacting Z0, and the nonlinearity of Zc. These effects and considerations will be discussed in this section.

Current Differential Schemes

Using current differential (87) schemes for protecting UG cables, commonly as part of the overall protection package, is preferred because it is less affected by the more variable traits of cables and is not impacted by power swings. In current differential

schemes, the current that flows from the local terminal is compared to the current going into the remote terminal using a digital communication channel such as with optical fiber interfaces (IEEE C37.94), to determine if the fault is inside or outside the zone of protection for the cable [1, 2]. In UG cable protection, special consideration needs to be given to the charging current and the effects of shunt reactors, used to provide part of that current, through desensitization of the settings to prevent mis-operations [5]. Current differential schemes also need other protection elements to provide backup since they only consider current values and are susceptible to mis-operating in the event of CT saturation [1].

Directional Comparison Schemes

Another protection scheme that is commonly used alongside other schemes in protecting UG cables is directional comparison (DCB/POTT) which use phase, ground, and zero-sequence, and/or negative-sequence directional elements to determine if a fault is in the protection zone based on whether the fault direction at the two ends of the protected cable are in agreement [1,2]. Directional protection schemes use both voltages and currents and need a communication channel, such as using fiber optic interfaces (IEEE C37.94), to transmit and receive directionality information from the relay at the other end of the cable [1,2]. In the event of a loss of communication, directions protection will still be valid locally at each end of the line [1]. To make directional comparison schemes more robust against UG cable's Z0 nonlinearity, negative-sequence directional elements could be used in place of ground directional elements [1]. Charging current can negatively impact directional element operations especially during line energization and open-pole conditions [5]. Therefore, other backup protection schemes improve reliability and security.

Phase Comparison Schemes

Phase comparison schemes are also commonly used in cable protection and are relatively similar to current differential protection, both using communication channels to exchange information between the local and remote terminals and primarily using current values. Phase comparison schemes take the current phase angles at the two ends of the cable and use either per-phase (segregated) or sequence current (composite) currents to compare between the local and remote terminals to determine internal faults based on the protection settings per the system characteristics [1]. Though phase comparison schemes can be less sensitive than current differential schemes, they can still be affected by charging current whose effects need to be considered when designing the scheme [5].

Distance Elements

Distance elements are often used in directional comparison schemes. However, the specific electrical characteristics of UG cables need to be carefully considered when setting distance relays. Due to the larger shunt capacitance of cables, the Z0 angles can be much smaller compared to overhead lines which creates the need for a larger range for the Z0 angle compensation setting [1].

Split-phase sections of the line can lead to nonlinear impedance responses. Creating the need for a greater reach of the overreaching distance elements to detect internal faults especially for faults that are farther from the protection terminal [2].

The return paths of underground cables also heavily depend on how the sheath is grounded and bonded as well as other possible return paths from nearby conductive structures such as railroads, fences, and pipes. These variabilities make Z0 nonlinear [1]. By nature of their layout, most cable faults concern a form of grounded fault. Thus, it is

important to account for these effects when setting distance relays, such as when calculating the compensated ground loop impedance [1].

$$Z_C = \frac{V_a}{I_a + K_0 + I_r} \tag{1.2}$$

The compensated ground loop impedance relies on the zero-sequence current compensation factor (k0), shown in equation (1.3), to properly set distance relays [1].

$$k_0 = \frac{Z_{0L} - Z_{1L}}{3Z_{1L}} \tag{1.3}$$

In modern digital relays, different zero-sequence current compensation factors can be set for each zone of protection with wider magnitude and angle ranges. Digital relays also provide settings to correct nonlinear line angles with the aim of avoiding underreach and overreach of ground distance elements [4].

Given the lower series impedance of cables, the positive sequence impedance can be considerably smaller than that of overhead lines. If the cable length is short enough, the cable's Z1 may be out of range for the relay settings [1].

Given that most underground cable faults tend to be permanent and can cause serious damage to the cables through extreme heat generation and arc flash burns, fast protection operation and blocking reclosing are crucial to prevent further damage especially in mixed systems with overhead and underground lines.

1.5 Fault Location Identification

Underground cables' unique electrical characteristics make them harder to model and protect. This holds true for detecting fault locations as well, where the higher shunt capacitance and lower series inductance cause a Z1 which is greater than the Z0, and the many return paths, depending on how the cable is configured, lead to a nonlinear Z0. Mixed or hybrid lines which incorporate both overhead and underground section add greater

complexity given the inherent difference in the electric properties of each line section, principally the impedances and wave propagation velocities [2].

1.5.1 Impedance-Based Fault Location

The double-ended impedance-based fault locating method is typically more accurate than the single-ended method. Therefore, it will be used as the Z-based fault locating method throughout these studies. This method can use phase voltages, phase currents, and sequence components to calculate the fault location based on the equivalent circuit model shown in Figure 1.2 [6]:

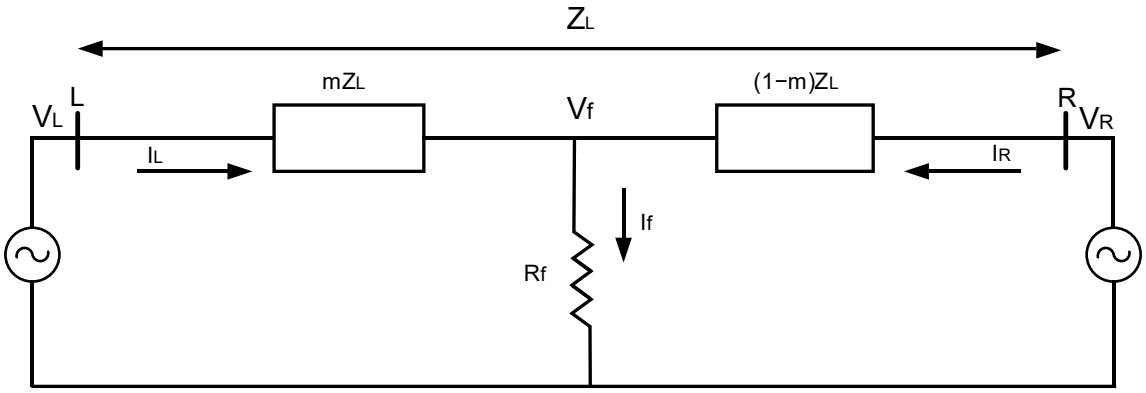

Figure 1.2 Fault on transmission line of a two-bus system

Voltages and currents at each terminal are measured and the line sequence impedances are set in the relay, with the exception of the fault location *m* and the fault voltage *Vf*. Equations (1.4) and (1.5) can be drawn based on Kirchhoff's voltage law [6]:

$$V_L = mZ_L I_L + V_f \tag{1.4}$$

$$V_R = (1-m)Z_L I_R + V_f \tag{1.5}$$

Then the equation for calculating the fault location *m* can be drawn:

$$m = \frac{V_L - V_R}{Z_L(I_L + I_R)} + \frac{I_R}{I_L + I_R} \tag{1.6}$$

The T401L relay's DE Z-based method is based on the sequence voltage principle that uses sequence voltages, sequence currents, and sequence impedances to calculate the fault location in balanced and unbalanced faults are shown in equations (1.7) and (1.8) respectively [7]:

$$m_{bld} = Real\left(\frac{V_{1L}-V_{1R}}{Z_{1L}(I_{1L}+I_{1R})} + \frac{I_{1R}}{I_{1L}+I_{1R}}\right) * LL \quad (1.7)$$

$$m_{ubd} = Real\left(\frac{V_{2L}-V_{2R}}{Z_{2L}(I_{2L}+I_{2R})} + \frac{I_{2R}}{I_{2L}+I_{2R}}\right) * LL \quad (1.8)$$

Where: V_{1L} and I_{1L} are the local terminal positive-sequence voltage and current
V_{1R} and I_{1R} are the remote terminal positive-sequence voltage and current
V_{2L} and I_{2L} are the local terminal negative-sequence voltage and current
V_{2R} and I_{2R} are the remote terminal negative-sequence voltage and current
LL is the total line length

1.5.2 Traveling-Wave Fault Location

The traveling-wave fault location method detects high-frequency wave incidents at the fault and uses the arrival time of the wave to calculate the distance to it. There are two primary methods of TW FL, single-ended and double-ended. Similar to Z-based FL, the DE method is much more accurate than the SE method, therefore it will be used in this paper as the TW FL method.

Based on field data from the *Protection Challenges for North America's First Combined Cable/Overhead Double-Circuit 500 kV Transmission Line With Mutual Coupling* paper, Traveling-Wave Fault Location is much more accurate than impedance-based fault location when dealing with underground cables given that it is less reliant on the sequence impedances their possible variable behavior [2]. TW FL depends on the wave propagation velocity in the line. UG cables typically have a line propagation velocity of

about 0.5c which is considerably slower than that of overhead transmission lines which propagate at nearly the speed of light [2].

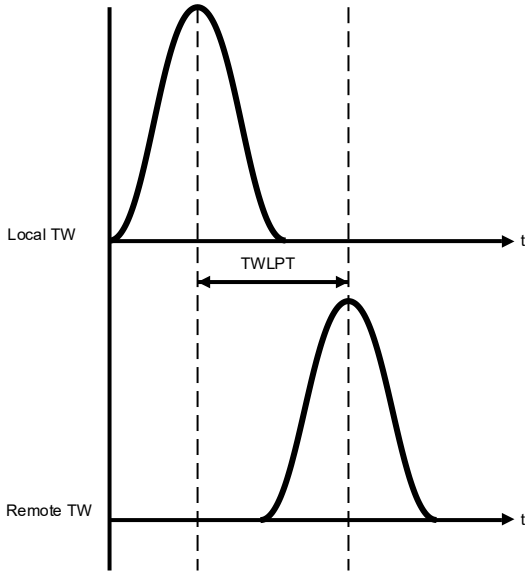

Figure 1.3 First TW incidents used for DE-TW TWLPT estimation

The DE TW fault locating method only considers the initial wave to the local and remote buses, as shown in Figure 1.3, which makes it more resilient to disruptions in reflected waves as used in the SE method. Equation (1.8) is used to calculate the fault distance [8,9]:

$$m = \frac{LL+(t_{L1}-t_{R1})v_p}{2} \tag{1.8}$$

Where: LL is the line length.

t_{L1} and t_{R1} are the first TW arrival times at the local and remote terminal respectively

v_p is the voltage propagation velocity

The fault location using DE-TW method can be represented in a Bewley diagram where the two ends are the two power system terminals and point *F* is the fault point the distance to which is to be calculated as represented in Figure 1.4 where m is the distance to the fault point from the local terminal.

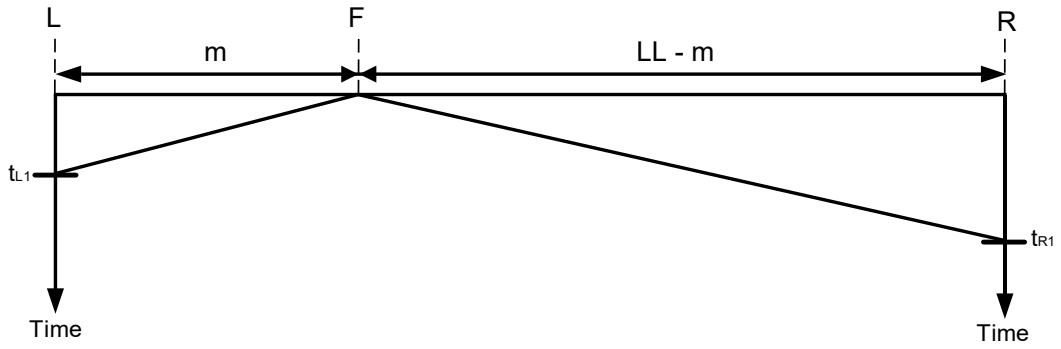

Figure 1.4 Bewley Diagram for DE-TW Fault Locating

Given the equation for the line propagation velocity (1.9), the fault location equation based on the Traveling-Wave Line Propagation Time (TWLPT), which is the setting value used by the relay, can be drawn as in equation (1.10) [10]:

$$v_P = \frac{LL}{TWLPT} \tag{1.9}$$

$$m = \frac{LL}{2}\left(1 + \frac{(t_{L1} - t_{R1})}{TWLPT}\right) \tag{1.10}$$

The TW FL method is strongly dependent on the propagation velocity of the line, therefore its calculation must be done with great care since errors introduced to it can manifest as large inaccuracies in the estimated fault location as the length of the line increases.

1.5 Organization of Thesis

The thesis is designed to first review all necessary background information related to the topics explored throughout, then explain the testing setup in detail and finally analyze the results. Initially, a general overview of UG cables, their protection and fault location is discussed. A detailed examination of all relevant UG cable configuring criteria is then performed and expanded on. The fault characteristics suspected to affect the accuracy of the DE-TW and DE-Z FL methods are reviewed next. Then the methodology and tools

used for testing each FL method's accuracy in UG cable faults are discussed with practical notes on setting up the HIL tests. Next, all collected results are analyzed, and all findings are explained with reference to the concepts previously discussed and all relevant data presented for further investigation. Finally, the full scope of the thesis is reviewed and summarized to conclude the research.

CHAPTER 2: UNDERGROUND CABLE CONFIGURATION CONSIDERATIONS

There are a multitude of factors affecting the electrical characteristics of UG cables, which include but are not limited to cable sheath grounding and bonding method, cable laying method, core transposition, proximity to other structures (especially metallic structures), and ground resistivity [11]. Considering the research scope and simulation limitations, the parameters tested consist of the cable transposition with cross-bonded sheaths laid out in a trefoil formation.

2.1 Cable Configuration Factors and Limitations

When simulating/modeling an XLPE type cable, some of the most fundamental parameters that need to be well identified are [1,12]:

- The conductor type as it pertains to the resistivity and permeability of the material.
- The conductor's inner (if hollow inside) and outer radius.
- The number of insulation layers and the insulator material's permittivity and permeability.
- The inner and outer radii of the respective insulator layers.
- The sheath material's resistivity and permeability.
- The sheath's inner and outer radii.
- Whether the sheath is grounded, cross-bonded, or ungrounded.
- The transposition of the cables.
- How the cables are laid out (ex: Trefoil) and their distances/coordinates with respect to each other.
- The armor's resistivity and permeability (if applicable to the cable).

- The armor's inner and outer radii.
- Whether the armor is grounded or transposed.
- The outer conductor's resistivity and permeability (if applicable to the cable).
- The outer conductor's radii.

2.2 Cable Bonding and Grounding Methods

One reason for the fundamental difference between overhead lines and underground cables is the metallic screen/sheath grounding and bonding which provide a return path for the charging current, conduct fault current, control sheath voltages, and limit losses and thermal stress [13].

AC current flowing through XLPE cables with a single conductor, induces a secondary voltage on the sheath layer which can cause surge protection challenges. In three-phase circuits, bonding the sheaths of the three cables leads to a circulating current in the sheath layer that leads to losses. Different sheath bonding and grounding methods are done to reduce or remove induced voltages and losses on the sheath as well as to provide a path of return for fault currents [14].

2.2.1 Single-Point Bonding and Grounding

Single-point binding is done when sheaths of the three cables are bonded together and grounded at either end of the cable or midway through the cable length. As there is no closed loop circuit, there is no circulating current along the cable sheath. Therefore, losses and heat generation are mitigated. However, induced voltages will exist along the cable, increasing at points further from the grounded point [1].

2.2.2 Solid Bonding and Grounding

The cable sheaths can be bonded together at both ends (Solid Bonding) which helps with removing the induced voltages on the sheath. This creates a closed loop for the sheath current which generates significant heat lowering the cable's load carrying capacity [1].

2.2.3 Cross Bonding and Grounding

Cross bonding the cable sheath helps with eliminating the induced voltage on the sheath by equalizing the potential of the sheaths for each cable/phase. This helps reduce the circulating current in the sheaths which lowers losses and increases the cable's load bearing capacity. The details of how cross bonding is done can vary, especially for longer cables. In general, cross bonding cables includes sectionalizing them in minor and major sections as shown in Figure 2.1 [4]. Each major section is made of three minor sections of equal length that are cross connected at each minor section. Sheaths on each end of the major sections are bonded and grounded to eliminate the sheath's induced voltage which can only be achieved when the cables are in trefoil formation or transposed [1,14].

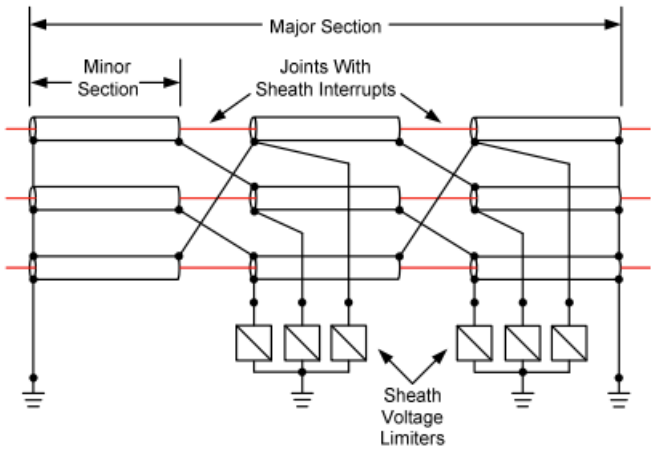

Figure 2.1 Cable Cross Bonded Configuration [1]

2.3 Cable Layout Method

The two prominent cable laying formations are flat formation and trefoil formation. In the flat formation, cables are laid laterally spaced from each other which helps with heat dissipation thus increasing its load capacity. However, this formation comes at the cost of discontinuous impedances and asymmetrical mutual inductance and capacitance which leads to additional modeling and protection complexities [13]. It has been shown that flat-laid cables exhibit the largest ground loop reactance discontinuities, particularly when untransposed [11]. The trefoil formation arranges the conductors in a triangular geometry which improves electromagnetic balance of the cable, lowering the mutual asymmetry and thus reducing the ground loop impedance discontinuities [13].

Underground cables can be either directly buried or installed in underground tunnels. Tunnel installations provide improved geometric symmetry, reducing electromagnetic imbalances [13]. The layout formations studied by the "*High voltage AC underground cable systems for power transmission – A review of the Danish experience"* paper, the tunnel trefoil cables layout with transposition shows the smallest ground loop impedance discontinuities [11].

The cable's physical layout and transposition mainly impact the positive-sequence impedance of the line as it affects the mutual inductance and capacitances between the conductors/phases. Given that the positive-sequence and/or the negative-sequence impedances are used in all short circuit calculations, careful considerations for how the cable is physically configured is crucial for modeling/simulating it accurately.

CHAPTER 3: FAULT CHARACTERISTIC CONSIDERATIONS

Different fault characteristics and conditions can also greatly influence the effectiveness of protection schemes and fault location estimation accuracy. Some of the most common and impactful fault characteristics are the fault type (phases involved), fault resistance, fault location (on the line or on equipment), and the point-on-wave of the fault occurrence. There are other criteria that affect fault behavior, but for the sake of simplifying these preliminary studies, the aforementioned characteristics will be the main criteria by which the studies will be conducted.

3.1 Fault Type

Phase to ground faults are the most common form of fault on underground cables given their inherent proximity to the earth [1]. In overhead lines, the order of commonality amongst fault types follows as such: phase-ground, phase-phase, 2-phase-ground, 3-phase [15]. From this, it can be inferred that underground cables would follow a similar pattern, bearing in mind that the vast majority of faults would include the ground. Therefore, the impact of different fault types, especially those involving the ground, needs to be well studied and understood, to perform accurate fault location estimation. In this study, all faults will be permanent and non-evolving.

3.1.1 Phase-Ground Faults

A phase to ground fault involves a short between one of the three phases of the transmission line and the ground through a resistance R_f. Given that in the symmetrical method load currents are ignored, the current in the unfaulted phases will be zero. Thus, the sequence currents for an AG fault can be calculated using equation (3.1) [16].

$$\begin{bmatrix} I_0 \\ I_1 \\ I_2 \end{bmatrix} = \frac{1}{3}\begin{bmatrix} 1 & 1 & 1 \\ 1 & a & a^2 \\ 1 & a^2 & a \end{bmatrix}\begin{bmatrix} I_a \\ 0 \\ 0 \end{bmatrix} = \frac{1}{3}\begin{bmatrix} I_a \\ I_a \\ I_a \end{bmatrix} \tag{3.1}$$

The phase-ground sequence network circuit can be drawn as shown in Figure 3.1 where the positive, negative, and zero-sequence networks are connected in series with the return going through three-times the fault resistance [16].

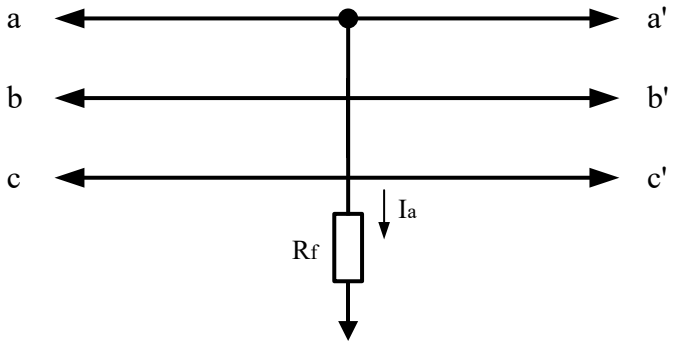

(a)

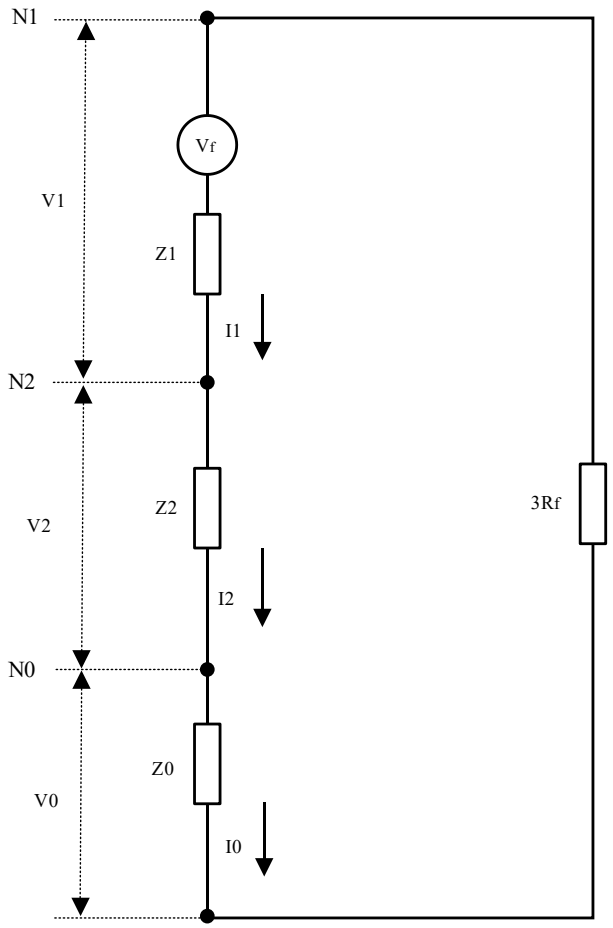

(b)

Figure 3.1 Phase-Ground Fault (a) On Three-Phase System (b) Sequence Network

Based on circuit analysis on the sequence network and derivations from equation (3.1), the following equations can be drawn [16].

$$V_f - I_1 Z_1 - I_2 Z_2 - I_0 Z_0 = 3R_f I_0 \tag{3.2}$$

$$I_f = I_a = \frac{3V_f}{Z_1 + Z_2 + Z_0 + 3R_f} \tag{3.3}$$

The equations for the fault current indicate the reliance of phase-ground faults on all sequence impedance components. Therefore, the effects of all fault and cable characteristics that affect the positive/negative and zero-sequence impedances will be studied through the application of Ph-Gnd faults.

3.1.2 Phase-Phase Faults

Phase-to-phase faults can occur between any two phases through a fault resistance R_f. The current from such faults circulates between the affected phases and flows back to the source, while the fault current in the unfaulted phase is zero. For example, the sequence currents can be calculated as shown in equation (3.4) for a BC fault [16].

$$\begin{bmatrix} I_0 \\ I_1 \\ I_2 \end{bmatrix} = \frac{1}{3}\begin{bmatrix} 1 & 1 & 1 \\ 1 & a & a^2 \\ 1 & a^2 & a \end{bmatrix}\begin{bmatrix} 0 \\ I_b \\ -I_b \end{bmatrix} = \frac{I_b}{3}\begin{bmatrix} 0 \\ a - a^2 \\ a^2 - a \end{bmatrix} \tag{3.4}$$

The phase-phase sequence network circuit is shown in Figure 3.2 where the positive and negative-sequence networks are connected in parallel through the fault resistance [16].

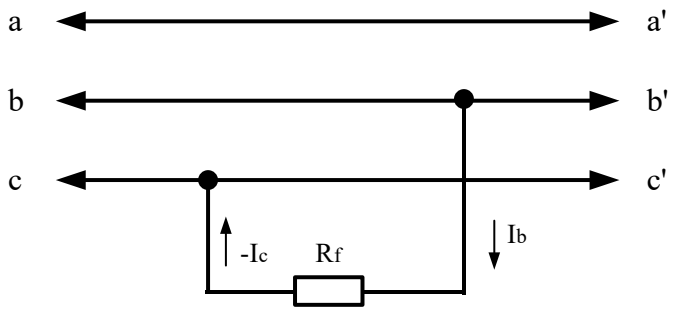

(a)

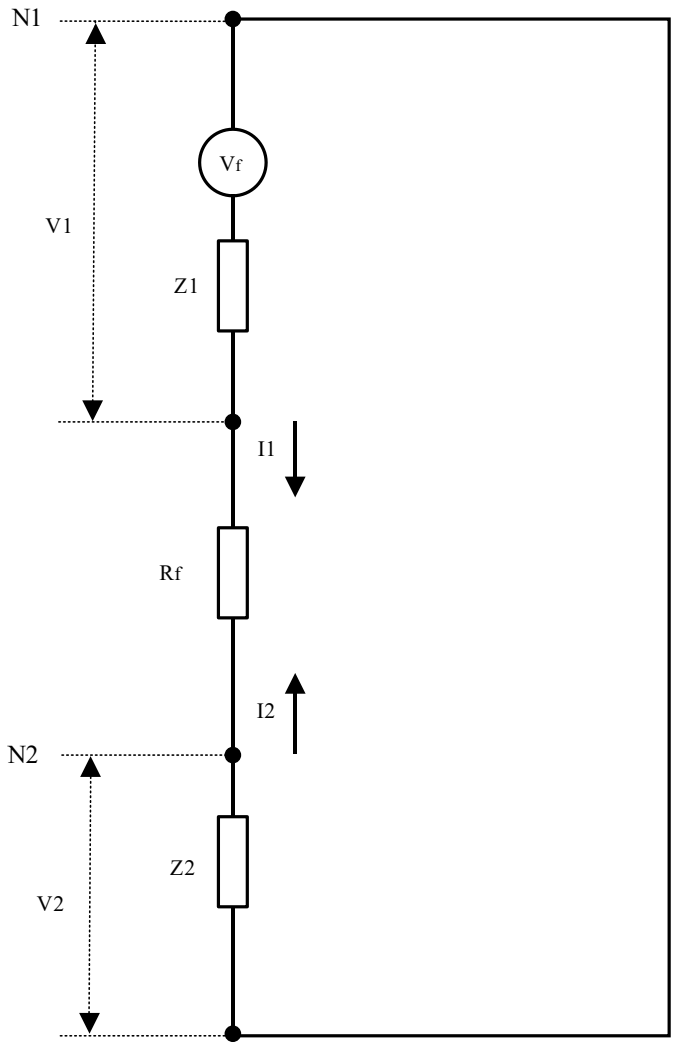

(b)

Figure 3.2 Phase-Phase Fault (a) On Three-Phase System (b) Sequence Network

Based on the sequence network circuit, equation (3.5) can be set up, and equation (3.6) is drawn from equation (3.4), from which the equation for the phase current with respect to the system voltage and impedances can be made (3.7) [16].

$$I_1 = -I_2 = \frac{V_f}{Z_1+Z_2+R_f} \tag{3.5}$$

$$I_b = -I_c = (a^2 - a)I_1 = -j\sqrt{3}I_1 \tag{3.6}$$

$$I_f = I_b = -\frac{j\sqrt{3}V_f}{Z_1+Z_2+R_f} \tag{3.7}$$

3.1.3 Double-Phase-Ground Faults

Faults between two phases and the ground are known as double Phase-to-ground faults which can result in a fault current flowing from the two phases through a fault resistance R_f to the ground. For an ABG fault, for instance, the sequence voltages can be calculated using equation (3.8) using the identity $V_b=V_c$ given that they are short-circuited together [16].

$$\begin{bmatrix} V_0 \\ V_1 \\ V_2 \end{bmatrix} = \frac{1}{3}\begin{bmatrix} 1 & 1 & 1 \\ 1 & a & a^2 \\ 1 & a^2 & a \end{bmatrix}\begin{bmatrix} V_a \\ V_b \\ V_b \end{bmatrix} = \frac{1}{3}\begin{bmatrix} V_a + 2V_b \\ V_a + (a^2 + a)V_b \\ V_a + (a^2 + a)V_b \end{bmatrix} \tag{3.8}$$

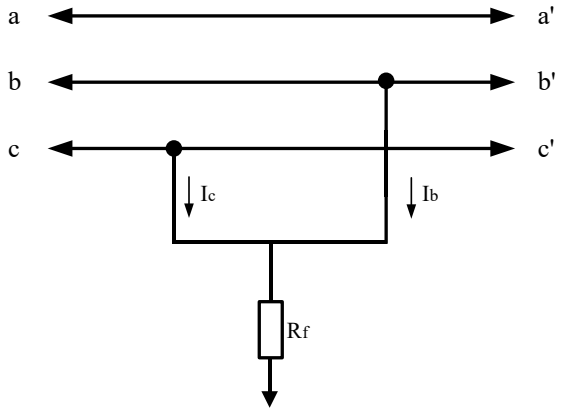

(a)

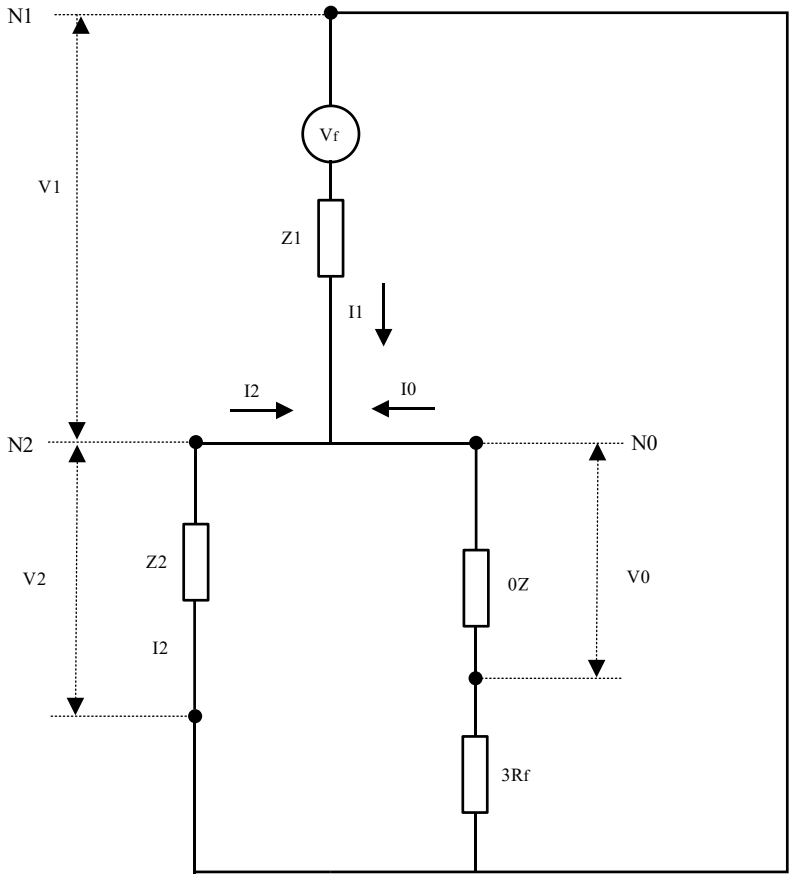

(b)

Figure 3.3 Double-Phase-Ground Fault (a) On Three-Phase System (b) Sequence Network

Based on the sequence network circuit shown in Figure 3.2, it can be concluded that Z_1 is in series with the parallel combination of Z_2 and Z_0+3Z_f. Thus, equation (3.9) can be made to calculate for the positive sequence current I_1, which is the sum of I_2 and I_0 [16].

$$I_1 = \frac{V_f}{Z_1 + \frac{Z_2(Z_0+3Z_f)}{Z_2+Z_0+3Z_f}} \tag{3.9}$$

3.1.4 Three-Phase Faults

Three-phase faults are symmetrical faults which occur between the three phases, with a fault resistance R_f between each of the two corresponding phases as shown in Figure 3.4 (a). Given the balanced nature of these faults, phase voltages are calculated as in equation (3.10) and based on the equivalent sequence network of these faults, shown in Figure 3.4 (b), equations (3.11) and (3.12) can be drawn [16] since I_1 is the only current flowing in symmetrical circuits.

$$\begin{bmatrix} V_a \\ V_b \\ V_c \end{bmatrix} = \begin{bmatrix} Z_f & 0 & 0 \\ 0 & Z_f & 0 \\ 0 & 0 & Z_f \end{bmatrix} \begin{bmatrix} I_a \\ I_b \\ I_c \end{bmatrix} \tag{3.10}$$

$$I_1 = \frac{V_f}{Z_1 + Z_f} \tag{3.11}$$

$$\begin{bmatrix} I_a \\ I_b \\ I_c \end{bmatrix} = \begin{bmatrix} 1 & 1 & 1 \\ 1 & a^2 & a \\ 1 & a & a^2 \end{bmatrix} \begin{bmatrix} 0 \\ I_1 \\ 0 \end{bmatrix} \tag{3.12}$$

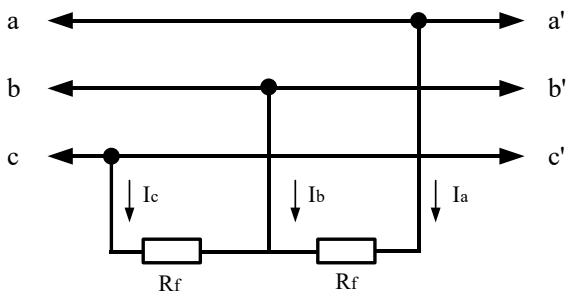

(a)

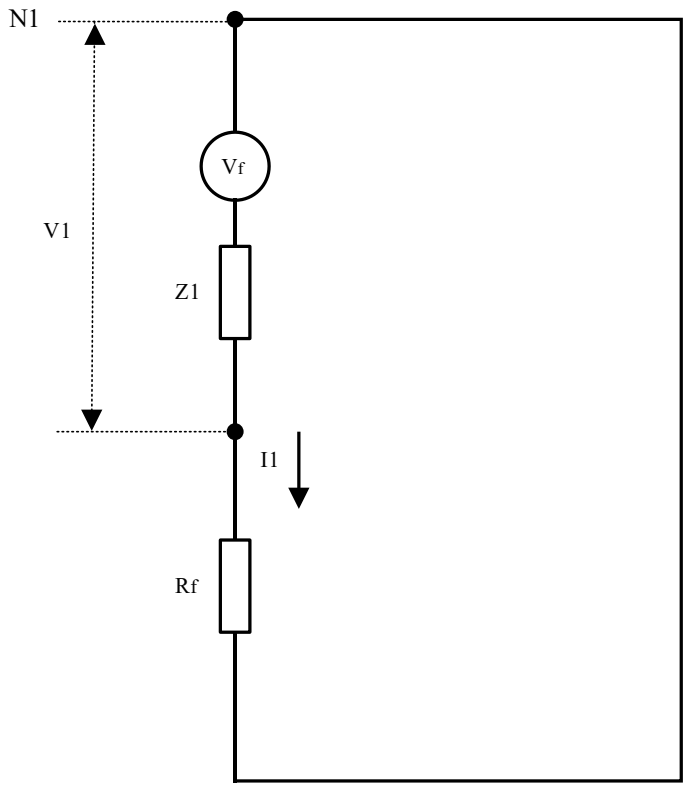

(b)

Figure 3.4 Three-Phase Fault (a) On Three-Phase System (b) Sequence Network

3.2 Fault Location

The fault current and voltage behavior depend heavily on the distance of the fault from the measurement terminal(s). In general, the metered fault currents decrease, and fault voltages increase as a factor of distance from the measuring terminal as a result of the line impedance accumulating as a factor of distance. Due to the fault location's effects on the apparent impedance, typically fault locating errors rise as a result of the faults being closer to the terminals [17]. Larger shunt capacitances of UG cables also affect the fault characteristics based on the location of the fault depending on how the cables are bonded and grounded.

To consider the effects of the fault location on the accuracy of the fault locating estimation errors, three spots along the cable length were considered for applying faults:

25%, 50%, and 75% of the line. These fault locations were chosen to equally divide the cable length and study the effects of FL on the estimation accuracy as a factor of proximity to the metering terminal in conjunction with other fault and cable characteristics.

3.3 Fault Resistance

As discussed in the *Fault Type* subsection, fault resistance can affect the equivalent sequence impedance of all fault types and can greatly impact the fault current magnitude. Therefore, three sets of fault resistances were chosen for these studies to demonstrate the possible impact(s) of a low (0.01 Ω), medium (1 Ω), and high (100 Ω) fault resistance on the TW and Z-based fault location estimation performance. Theoretically, higher fault resistance should lead to relatively smaller fault currents, the effects of which on the magnitude of the alpha and beta currents for TW FL will be investigated under different fault scenarios. For the sake of constraining the complexities of these initial studies, and to comply with most real-world events, fault impedances were considered to only include a resistive component.

3.4 Point-On-Wave

The point at which the fault occurs on the AC waveform can affect the transient behavior of the fault which could impact the performance of FL estimation depending on the method. Energy of traveling-waves, especially that of the first TW incident, strongly depends on the point at which the fault occurred along the waveform or the “fault inception angle” according to the *squared sinusoidal function* [18].

Each fault type can have a different wavefront energy which could impact the TW FL based on the combination of the fault type and POW of the fault incidence. For instance, Ph-Gnd faults could be more susceptible to insufficient wavefront energies compared to

Ph-Ph or 2-Ph-Gnd faults which typically are stronger and have two phases involved in case one phase is close to the zero-crossing point [18].

Therefore, as another factor for consideration, three general points along the waveform were chosen to be studied, the top of the waveform, the middle of the waveform, and the zero-crossing point. The rarity of faults occurring at the zero-crossing point has been noted, however for the sake of theoretical studies it was included as one of the points to study its effects. The POW was applied to the voltage waveform at each fault location. Based on the specifics of its implementation into the simulation model, the points are not exactly at the same point for all cases; they are in the general vicinity of the *top* and *middle* of the waveform, to help identify the general effects of POW of the fault on the accuracy of the fault locating methods.

CHAPTER 4: HARDWARE-IN-THE-LOOP SIMULATIONS

4.1 Tools

Throughout this paper, a hardware-in-the-loop (HIL) system was devised to test the fault location estimation functionality of an industry-standard device in a simulated power system model. Simulations were done using the *Real-Time Digital Simulation* (RTDS) simulator along with the *Real-Time Simulation Control and Data Acquisition* (RSCAD) simulation software, the power system designed to test the fault location estimation functionalities under different circuit and fault conditions. The device used for testing the fault location estimation function was the SEL-T401L which is an ultra-high-speed line relay with time-domain line protection capabilities.

4.1.1 RTDS/RSCAD

Real-time simulations of the underground cables in a simple two-bus power system were done using RTDS which models the electromagnetic transient behavior of cables under different fault conditions. An RTDS rack with three cores simulated the power system and controlled two GTAO (Gigabit Transceiver Analogue Output) cards to send analog voltage and current signals to the relays. The graphical user interface used to create and run these simulations was the RTDS proprietary software RSCAD which models the power system equipment, the control diagrams, and hardware used to send and receive signals [19].

4.1.2 SEL-T401L

The SEL-T401L relay was used due to its fault location estimation capabilities using traveling-wave technology as well as impedance-based fault location. Using two T401Ls, one at each end of the cable, allows for double-ended TW FL to be done through

a digital communication channel with a direct fiber optic channel or the more reliable IEEE C37.94 encoding. The T401L can perform ultra-high-resolution transient recording on a total of 6 current and 6 voltage channels with a 1 MHz sampling rate. It also has COMTRADE (Common Format for Transient Data Exchange) file playback capabilities which allow for events recorded on other devices or generated by simulation software such as RTDS and ATP to be played on the relay imitating the power system conditions [10].

4.3 Simulation Considerations

There are many factors to consider when designing an HIL power system simulation, chiefly the integrity of the power system and cable models with respect to real-world conditions need to be established. To ensure the cable model's validity, the cable parameters were borrowed from the *Protection of High-Voltage AC Cables* paper which defines the physical and electrical parameters for a single-conductor XLPE cable in a 230 kV system laid in the trefoil formation. Modeling the cable in RSCAD with these parameters resulted in the same sequence impedance values as defined in the paper which gave the confidence necessary to conduct all tests on the model.

4.3.1 Cable Model

The Cable Constants Program of RSCAD can be used to model different cable types depending on their physical and electrical characteristics [12]. This program was used to model three XLPE cables in trefoil formation as shown in Figure 4.1.

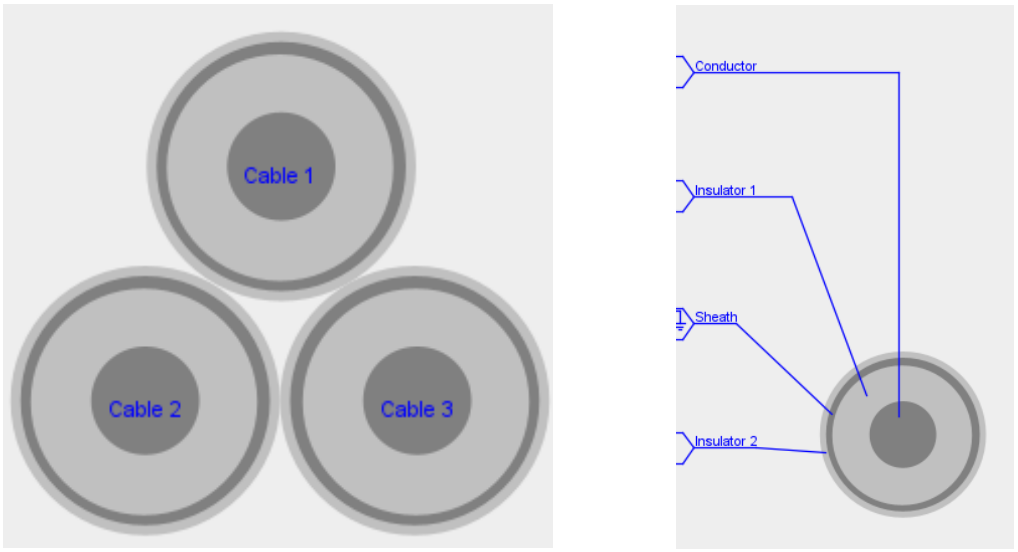

(a) (b)

Figure 4.1 XLPE Cable in RSCAD (a) Three Cables in Trefoil Formation (b) Single Cable Layers

The most relevant cable parameters which the program needs have been mentioned in section 2.1 notably each layer's electrical parameters and diameters. Other important criteria defined here are the length of the cable section, the ground resistivity, and frequency of the system (60Hz). The Model type used is the *Bergeron (Physical Data Entry)* to solve for the cable impedance matrices. The Bergeron model simplifies calculations by treating the resistive component of the cable as three lumped elements, a quarter of the total resistance at the two ends of the cable and half at the center all in series. Thus, neglecting the shunt conductance (G), the characteristic impedance equation is simplified from equation (4.1) to (4.2) [12].

$$Z_c = \sqrt{\frac{R+j\omega L}{G+j\omega C}} \tag{4.1}$$

$$Z_C = \sqrt{\frac{L}{C}} \tag{4.2}$$

Two crucial parameters used in the cable's modeling are the conductor transposition and sheath bonding/Grounding. These can be set individually for each cable

and affect the Z1 and Z0 of the cable respectively. The transposition and grounding/bonding methods are two of the parameters by which cable characteristics are tested under different fault conditions in these studies. The full configuration of the cable editor program along with the cable's electromagnetic and physical parameters are defined in Appendix A.

4.3.2 Power System Model

The simple 230 kV two-source power system connected through an UG transmission cable was modeled in RSCAD with a constant and balanced load flow between the Local and Remote terminals. The physical layout of the RSCAD model can be found in Appendix B. The cable lengths were divided into four sections to divide the line such that faults could be applied at three points along the cable, which as discussed previously were chosen to be 25%, 50%, and 75% of the line length. Figure 4.2 shows the general outline of the power system where the fault locations with respect to the Local terminal can be seen.

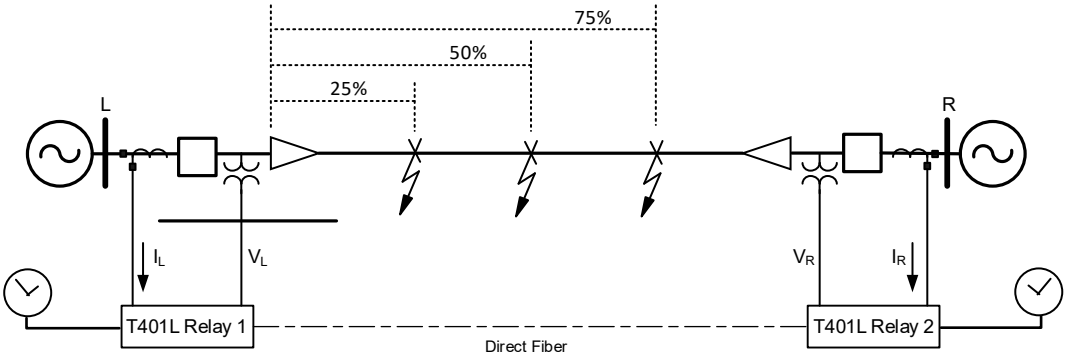

Figure 4.2: Power System Model with Fault Locations and T401L Relays

Given this transmission cable's short physical and electrical nature, the source-to-line impedance ratio (SIR) was chosen to be greater than 4 per the IEEE C37.113 guide for Protective Relay Applications to Transmission Lines [20]. Based on the realistic

steady-state load flow, cable ratings, and considerations for effects on the TW incident waveforms, the SIR was chosen to be around 8.

Metering is being done at the Local and Remote terminals where the respective voltage and current signals were sent to the relay through the GTAOs as low energy signals. The trip signal and breaker status bits are sent to the relay and breaker close bits were received from the relay through the GTFPI. The trip signal triggers the events on the relay to ensure that events are generated at the same time on both T401Ls. For the sake of avoiding unnecessary complexities, the *fault* signals generated an open breaker signal which opens the local and remote breakers after 3 cycles to mimic realistic power system conditions. Three cycles were chosen to account for an approximate 1 cycle relay operation delay and 2 cycle breaker operation delay. The *fault* signal also triggers the *trip* signal after 1 cycle. Through this, a standardized format of event report generation was designed to maintain consistency for the analysis to be done. Details of the RSCAD-HIL configuration can be found in Appendix C.

4.3.3 HIL Configuration

Connections between the RTDS rack and the T401Ls consist of analog and digital channels. The analog Voltage and Current connections from the RTDS GTAOs are connected to the T401L CTs and PTs. In the case of this study's setup, the T401L relays are specialized units which can take the low energy analog signals through a hardware setup that bypasses the CTs and PTs on the back of the relay, thus foregoing the need for an amplifier to amplify the low-energy signals to high energy secondary values. The digital connections are between the RTDS GTFPI and the binary inputs/outputs of the T401Ls. Figure 4.3 shows a high-level diagram of how the connections are set between RTDS and

each of the T401Ls. In Figure 4.4 (a) an example of the physical connections to the T401L is presented and Figure 4.4 (b) shows the corresponding connections to the GTAO card of the RTDS rack in the laboratory setup.

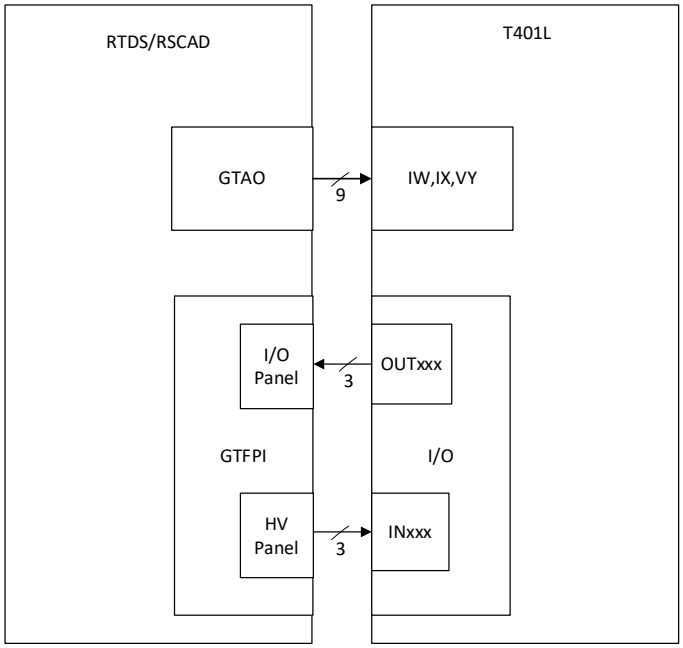

Figure 4.3 High-Level Connections Between RTDS Rack and T401L Relays

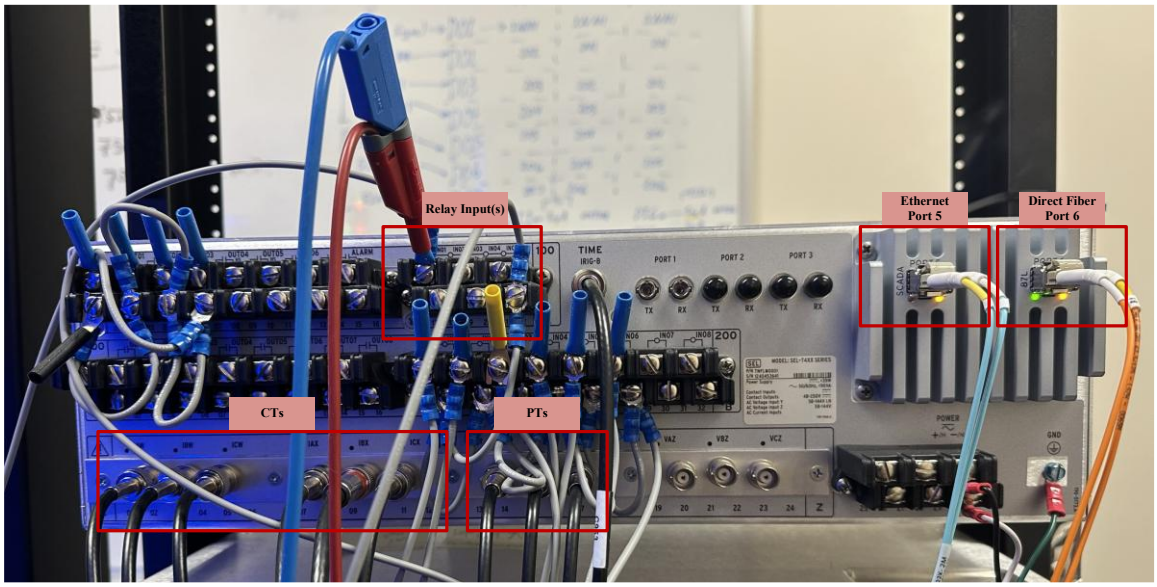

(a)

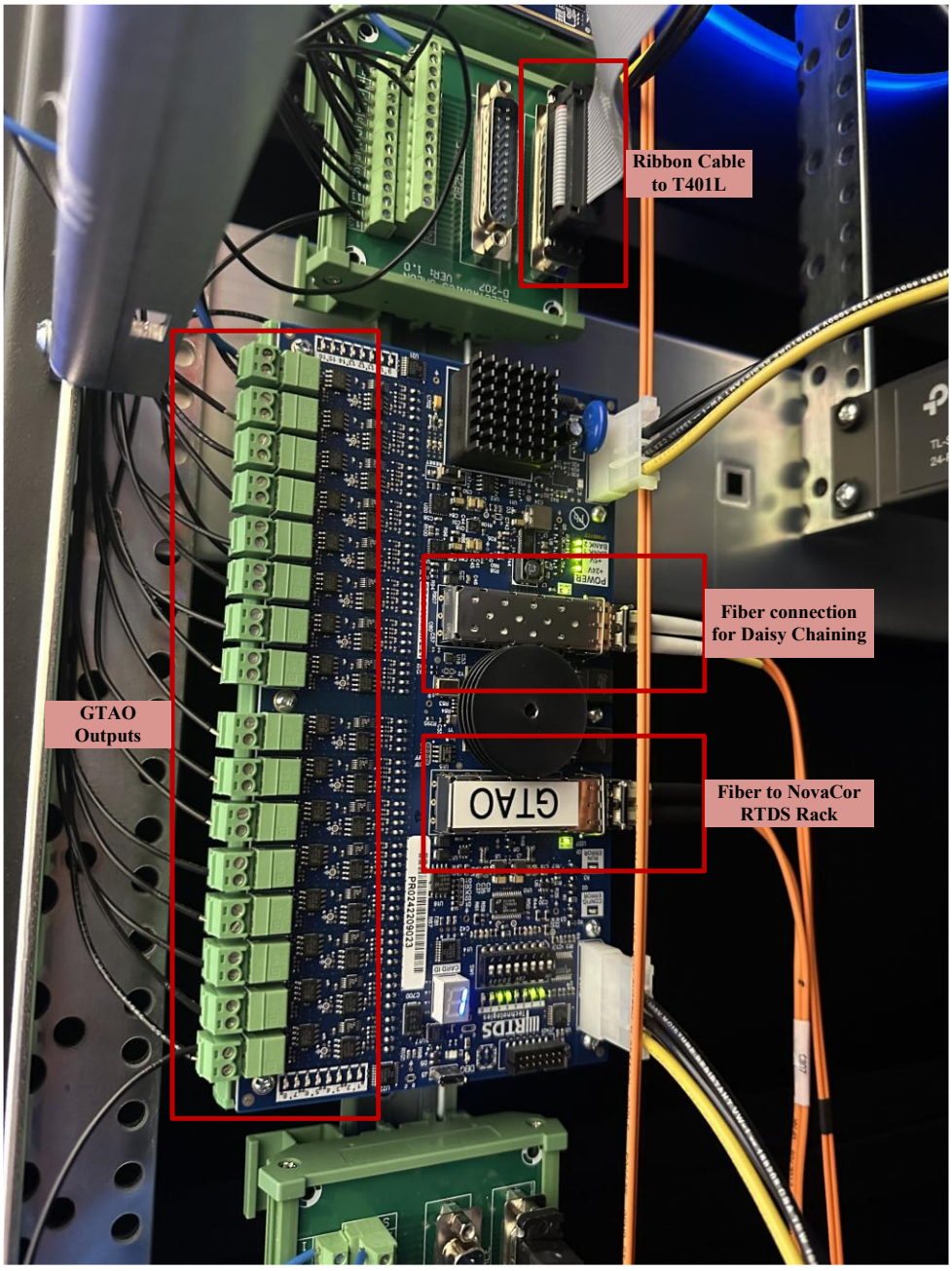

(b)

Figure 4.4 Physical Setup Connections; (a) On the T401L; (b) On the GTAO Card

4.4 Relay Settings Consideration

4.4.1 Settings Overview

Setting the T401L for effective double-ended traveling-wave and impedance-based fault location is crucial and involves a number of different steps and careful considerations. Given the general convention of using DE-TW for primary fault locating and DE-Z-based as the backup for UG cables, the settings discussed will include those required for both, some of which overlap. The full scope of the settings that were set and their values can be found in Appendix D.

Firstly, the power system settings need to be defined to provide the correct basis for any protection or fault location to be done correctly. There are more settings that can be set for more complex power systems, for applications to this simplified model, the settings include [10]:

AC Power System AC Inputs

- System nominal frequency and phase rotation.
- The CT(s) used to measure line currents and its/their CT ratios.
- The PT ratio and the secondary nominal voltage.

Line Configuration

- The total line/cable length along with the desired measurement units.
- The line's/cable's positive-sequence impedance magnitude and angle in secondary Ohms.
- The line's/cable's zero-sequence impedance magnitude and angle in secondary Ohms.
- The line/cable traveling-wave propagation time in microseconds (TWLPT).

Communications:

- Enable Port 6 used for direct fiber communication between the two T401Ls.
- Set the Transmit and Receive identifiers for each T401L.
- The Fault Locator Data Port setting needs to be set to the port used for fault location, in this case Port 6 given the use of direct fiber connection rather than C37.94 through Port 1.

Other advanced settings that can be helpful when dealing with cables are the TW cable propagation time (TWCPT) and the TW Mode. The TWCPT setting can aid with the DE-TW fault locating method's accuracy by performing time delay compensation present in CT and PT cables, if necessary [10]. The TW mode setting is an advanced setting which allows for the TW-based fault-locating method to be chosen as either CLARKE which is often used in overhead lines or conductors with bonded shields, or the PAHSE mode which is used for cables with isolated shields [10]. Since in all studies the cable's sheaths are cross-bonded, the CLARKE mode was used for all studies. Preliminary studies were conducted with both methods to establish certainty.

4.4.2 TW Line Propagation Time Calculation

The TW line propagation time for any cable can be found using the Energization Test whose steps are detailed out in the T401L instruction manual [10]. A general overview of the steps and special notes will be outlined here. A more detailed set of steps for how the test was performed in this case is described in Appendix E. To perform the energization test, first all breakers need to be open, and the system is fully deenergized, then only the local breaker is closed to generate traveling-waves through the system which cause disturbances that can be picked up by the relay through such relay word bits as TWDD.

The relay can be set to generate an event when a disturbance is detected. In the case of this setup where specialized low-energy input T401L units were used, the relays can pick up disturbances from noise. Therefore, an energization COMTRADE file needs to be generated from simulation software at a 1MHz sampling rate, converted to the *playback* file format, played back on the T401L to generate an event.

First, a similar power system model was made in RSCAD with the cable whose TWLPT intended to be calculated. It was noted that a power system with a relatively higher resistive component on the positive sequence source impedance aided in generating a higher incident wave to more easily identify the first TW times used in the DE-TW method. When using relays with high-energy inputs into CTs and PTs, the test can be directly run and an event generated based on the TWDD assertion.

When using low-energy input relays, the play back method may be necessary. Given the limitations on the number of RTDS cores available for modeling, the maximum simulation time stamp that could be used was 10us. Therefore, a COMTRADE event was generated at 100kHz in the RTDS model and upsampled to 1MHz using a MATLAB script. The 1MHz COMTRADE file was converted to the *playback* format using the *File Conversion Utility* available in the AcSELerator Quickset software. For accurate playback simulation, the event needs to have at least 50ms of steady-state pre-fault data. Therefore, the events were generated such that the circuit is initially in steady-state, then both remote and local breakers open, and once the system voltages and currents have stabilized at zero, the local breaker closes to initiate energization. The playback file was then re-played on the T401L using the *Playback Dashboard*.

The event generated on the relay was analyzed using the Bewley Diagram based on the alpha current TW. The time difference between the first incident wave and its reflection from the remote terminal is equivalent to twice the TWLPT time as shown in Figure 4.5 (a). Dividing this time difference by two results in the TWLPT value which in this case is 81.11ms. This TW propagation time can be used in the Bewley diagram to check the calculated time and to calculate the propagation velocity with respect to the speed of light which is generally considerably slower in UG cables compared to overhead lines.

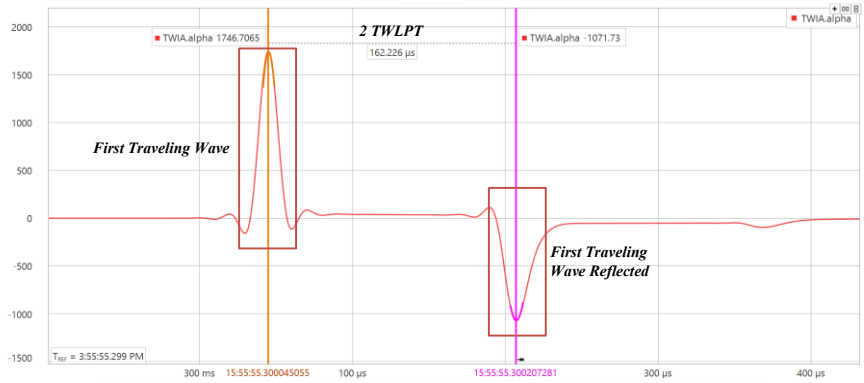

(a)

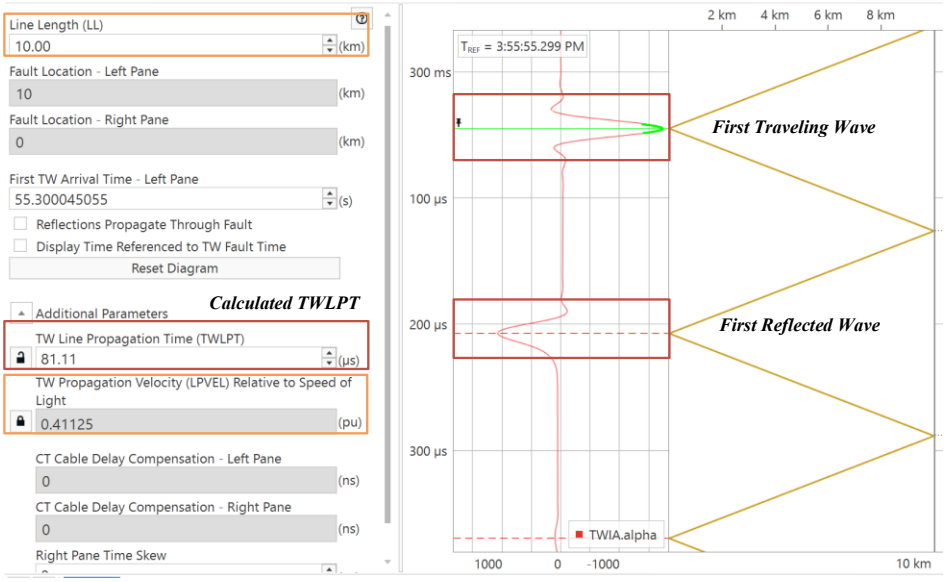

(b)

Figure 4.5 Energization Test (a) Alpha Current Analysis (b) Bewley Diagram Analysis

4.4.3 Line Sequence Impedance Estimation

The line sequence impedances can be found conveniently in the ".map" file generated from the RSCAD model once all cable parameters are entered correctly and the simulation is compiled. The equivalent Z1 and Z0 values are calculated for each cable section per the cable's length as shown in Figure 4.6 where "UG25" is the first 2.5 km section of the UG cable.

```
T-Line "UGC25" parameters at 60.00 Hz
Travel time(usecs) mode0 = 20.70471  mode1 = 20.60159  mode2 = 20.60159
CIRCUIT #1
    POSITIVE SEQUENCE
                    Line Impedance = 0.04 + j0.34 ohms
                                   = 0.34 /_82.61 degree
          Shunt Capacitive Reactance = 5668.79 ohms
    ZERO SEQUENCE
                    Line Impedance = 0.43 + j0.35 ohms
                                   = 0.55 /_38.78 degree
          Shunt Capacitive Reactance = 5668.94 ohms
```

Figure 4.6 Cable Sequence-Impedance Data from the .map File [12]

The Z1 and Z0 magnitudes will need to be adjusted for the full length of the cable and converted to secondary Ohms based on the CT and PT ratios used in setting the relay. More complementary information can be found in the "out" files generated for each cable section model.

CHAPTER 5: PROPOSED TESTING APPROACH IMPLEMENTATION

5.1 Overview

There are two main testing methods to run the intended studies: the Hardware-in-the-loop (HIL) method and the playback method. The playback method is possible on the T401L but is limited for large batch testing and does not have the capability of giving possible feedback/outputs to the power system. Therefore, the HIL method was chosen given its potential to be expanded for automated batch testing and real-time testing of the relay using RTDS.

All tests were run in a batch format while data such as the estimated fault location was collected from the T401L after each test case. The test automated cases consisted of an all-encompassing combination of fault-types, fault-locations, fault-resistances, and fault-points-on-wave. Different test runs were executed for the combination of cable configurations which affected the power system impedances and thus the relay settings. Therefore, each cable configuration had its respective set of initial settings which were sent to the relays at the start of each test case. Most notably, these settings include the system sequence impedances and the Traveling-Wave Line Propagation Time (TWLPT) of the cable configuration under test.

The data collected consisted of the Mega-Hz high-resolution (MHR) COMTRADES and the 10kHz (THR) COMTRADES and their respective header files. The MHR data contains the analog signals injected into the relay and importantly the alpha and beta waveforms which are used to determine the DE-TW FL based on the first incident wave time which can be plotted in a Bewley diagram for manual calculations and analysis. The TDR data contain processed analog signals, settings, and digital signals from the

relay's logic and operations mechanisms. The header file contains the estimated fault location for all methods, from which the DE-TW and DE-Z calculated fault locations are collected.

5.2 Examination Criteria

A quick overview of all test-cases with their corresponding fault and cable parameters used for testing can be found in Table 5.1 the details for which have been explained in the previous chapters.

Table 5.1 Test-Case Examination Criteria

Testing Category	*Testing Criteria*	*Testing Criteria Value*
Fault Characteristics	***Fault Type (10)***	AG, BG, CG, AB, BC, CA, ABG, BCG, CAG, ABC
	Fault Resistance (3)	0.01Ω, 1Ω, 100Ω
	Fault Location (3)	25% LL, 50% LL, 75% LL
	Point-on-Wave (3)	Top-of-Wave (90°-100°), Middle-of-Wave (110°-120°), Zero-Crossing (170°-180°)
Cable Characteristics	***Transposition (2)***	Transposed, Untransposed
	Bonding	Cross-Bonded
Fault Locating	***Fault Locating Method***	DE-TW, DE-Z
	FL Terminal	Local, Remote

5.3 Metrics

The percentage error for all cases will be calculated relative to the line length (10 km) as defined by the IEEE Standard C37.114 [21]:

$$\%\, error\ = \frac{|Estimated\ Fault\ Location - Actual\ Fault\ Location|}{Line\ Length} \tag{5.1}$$

All plots are based on the percentage error to standardize the errors for all results based on the cable length to achieve an objective analysis of all results regardless of the fault location. For practical purposes however, the actual errors in kilometers or miles are more intuitive. Therefore, the table summary of the averages for all cases will include the

percentage error as well as the actual distance error. This is especially important in longer lines where even the smallest of errors can lead to significant distances for the line workers who need to identify the exact fault location and will directly affect a utility's line re-energization time.

The T401L's DE-TW FL method has a reported accuracy of being within one tower span which is about 300m or 1000ft. The DE Z-Based method has accuracies of within 1-2 percent of the line-length [10]. All results will be gauged with respect to these expectations.

5.4 Case Study: Two-Bus System

The two-bus power system simulated to test the cable model in RSCAD was designed with simplicity in mind to avoid dilution of results due to other complex power system factors. It does, however, have the potential to be expanded in order to test the effects of more complex power system characteristics with cable models, such as transformers, shunt capacitor banks, series compensation capacitors, and more.

The two-bus system consists of two 230 kV sources at each terminal with a power flow angle of 5 degrees from the local to the remote terminal. The cable is divided into four equal sections of 2.5 km each where different faults can be applied at 25, 50, and 75 of the line. The current through the breakers at each terminal are metered by a non-saturable current transformer (CT) and the voltages are measured at each bus by potential transformers (PTs). The data from these CTs and PTs is sent to the relays as secondary metered values.

5.5 Results Analysis

To achieve a practical comparison between all sets of results, they were plotted in the following formation: One plot per each combination of fault-location and fault-point-on-wave, each plot divided into three fault-resistance subsections, each of which consist of the ten fault-types. The fault number on the x-axis represents the combination of fault-resistance and fault type. Plotted are the DE-TW and DE-Z-based percentage errors for cables that have transposed cores and cross-bonded sheaths (T-X) and cable that have untransposed cores and cross-bonded sheaths (UT-X). All results are based on the estimations of the T401L from the local terminal, which will always match exactly those of the remote terminal for DE-TW FL estimation and typically very closely for the DE-Z-based method. Each data point is the average of three fault events for each fault number to ensure the results are consistent.

5.5.1 Fault Characteristic Effects

The greatest fault characteristic factors affecting the percentage error in the FL estimation include the location of the fault, the fault-point-on-wave, and the fault type. All results analyzed in this subsection are for untransposed and cross-bonded cables. Only the fault characteristics are considered in these cases to make the impact of fault characteristics more visible. Plots with corresponding cable characteristics are included in the next subsection.

A clear pattern can be seen where the DE-TW FL method is more accurate or has relatively the same accuracy for faults closer to the terminals. While the DE-Z method is more accurate for faults at the middle of the cable line. This can be best observed in the

difference between Figures 5.1 and 5.2 with the accuracy of the two fault locating methods changing depending on whether the fault is at 25% or 50% of the line.

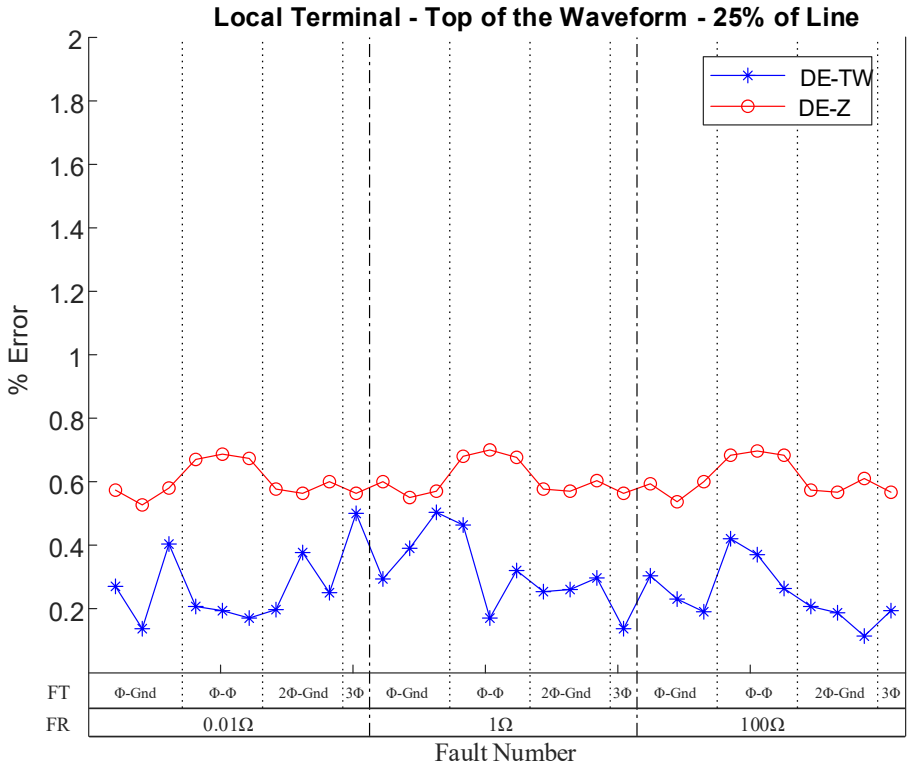

Figure 5.1 FL Error Comparison for TOW with Fault at 25% of Line

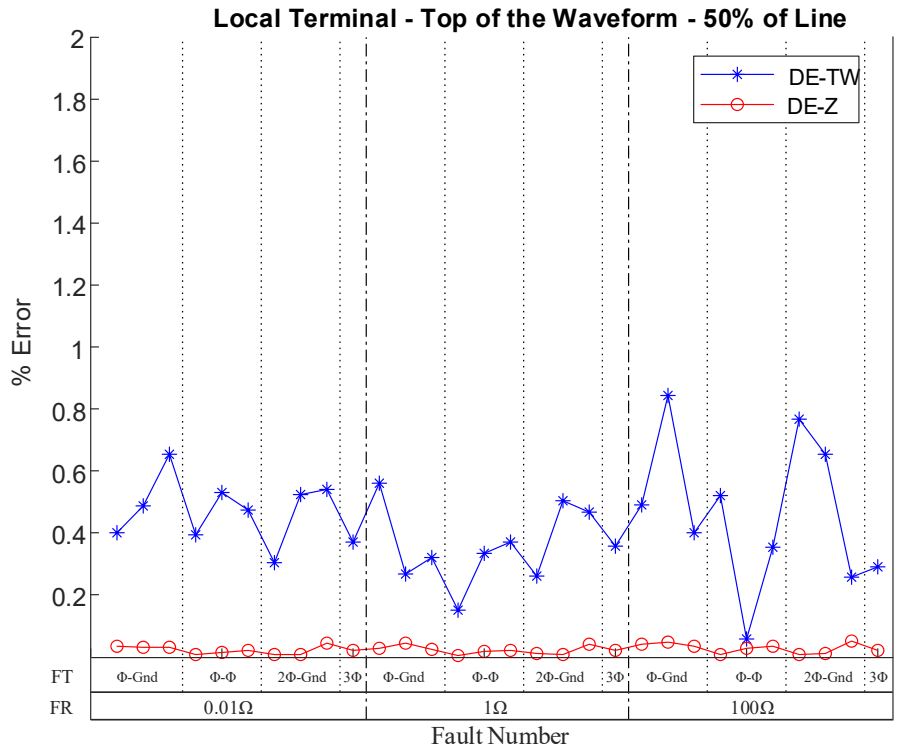

Figure 5.2 FL Error Comparison for TOW with Fault at 50% of Line

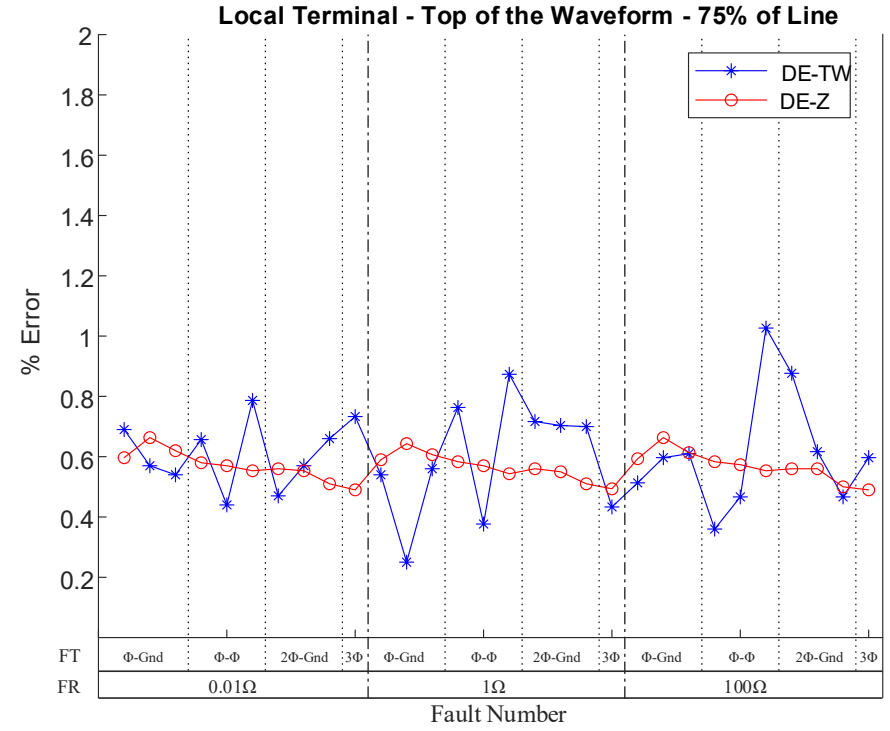

Figure 5.3 FL Error Comparison for TOW with Fault at 75% of Line

Based on the T401L's use of the negative-sequence voltage profile for DE-Z method, per equations (1.7) and (1.8), when the fault occurs near the middle of the line, phasor values of the negative-sequence voltages and currents will match relatively closely. As seen in the similarities between the I2 and V2 magnitudes and angles during the fault in Figures 5.4 and 5.5 where the red plots are from the local terminal and the green plots are from the remote. Figure 5.6 shows the metered voltages and currents at each terminal, and the fault location calculation based on the DE-Z method performed manually in SynchroWAVe using the equations shown in Figure 5.7.

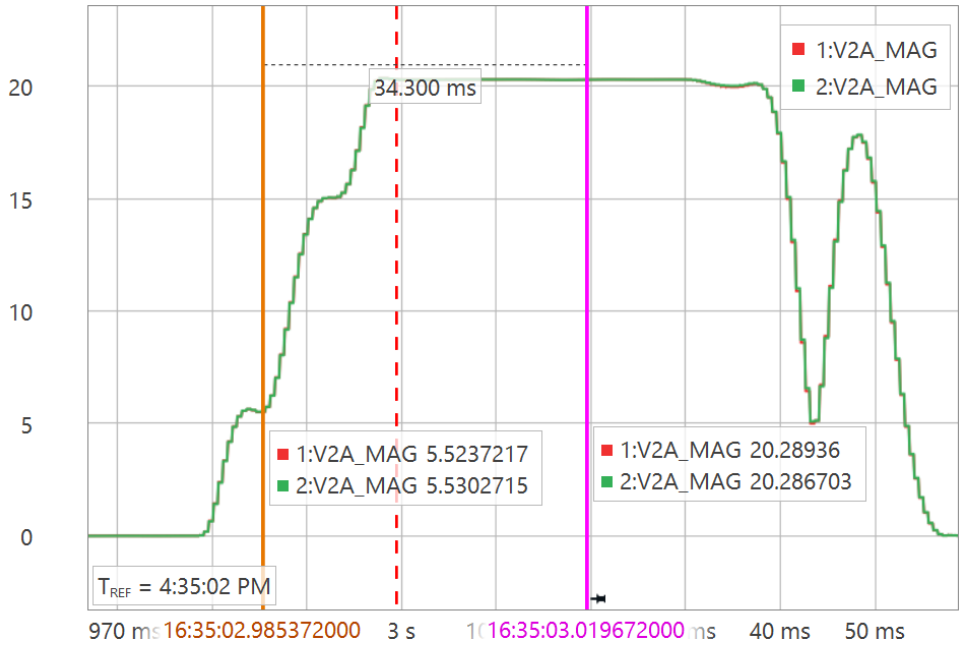

(a)

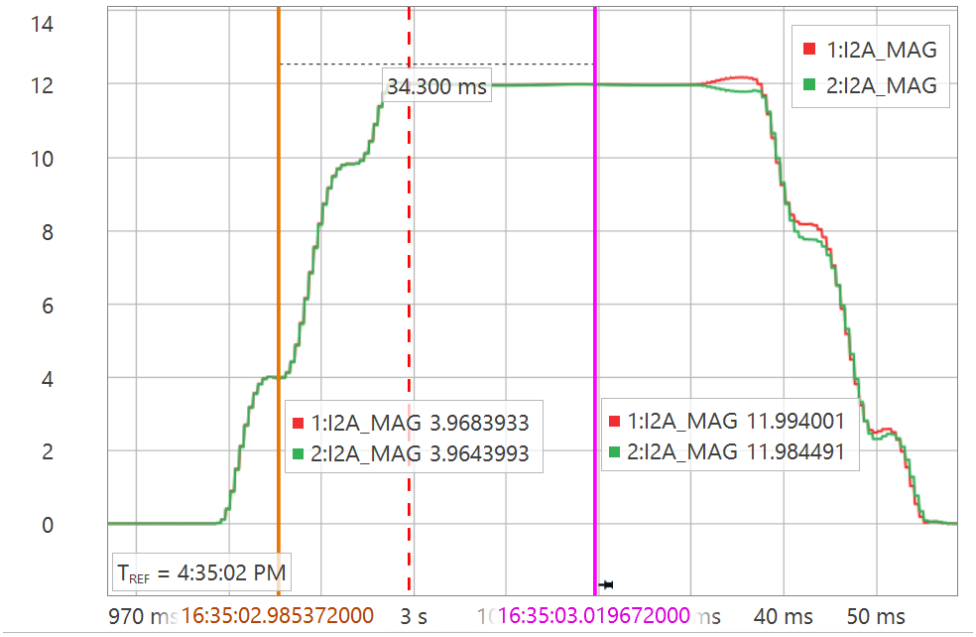

(b)

Figure 5.4 AG TOW Fault at 50% - Negative-Sequence (a) Voltage and (b) Current Magnitudes

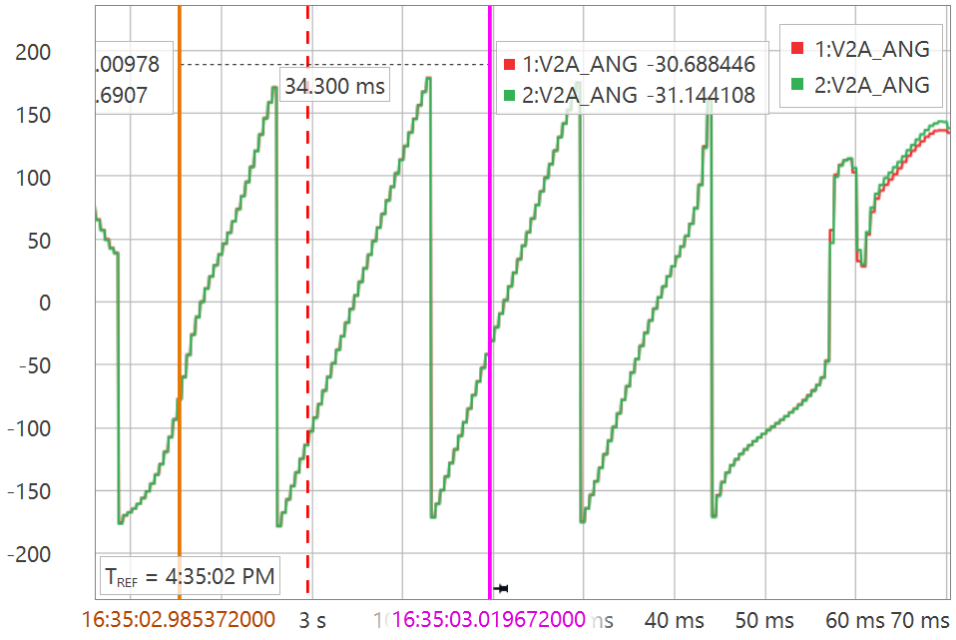

(a)

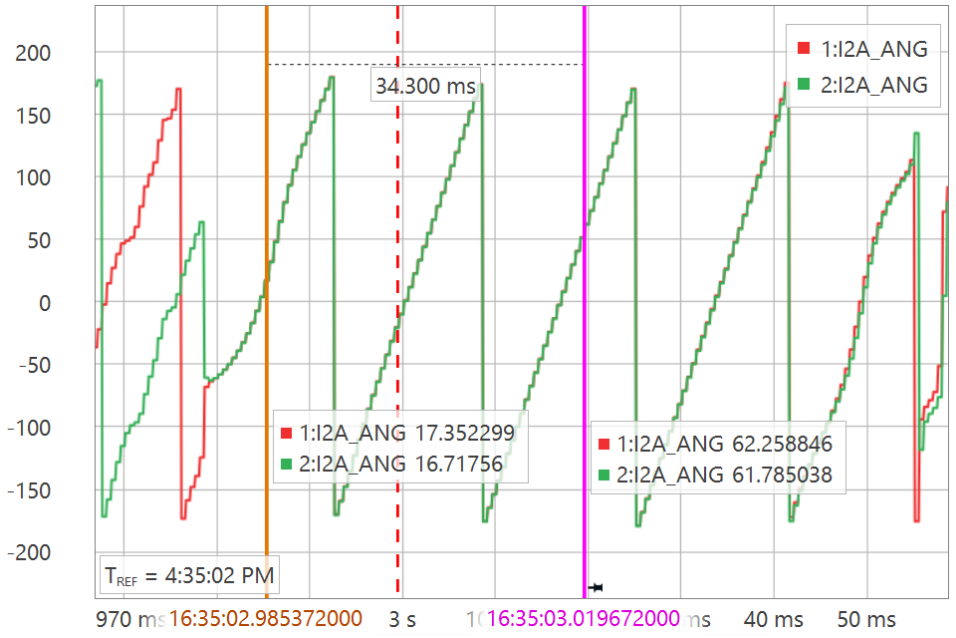

(b)

Figure 5.5 AG TOW Fault at 50% - Negative-Sequence (a) Voltage and (b) Current Magnitudes

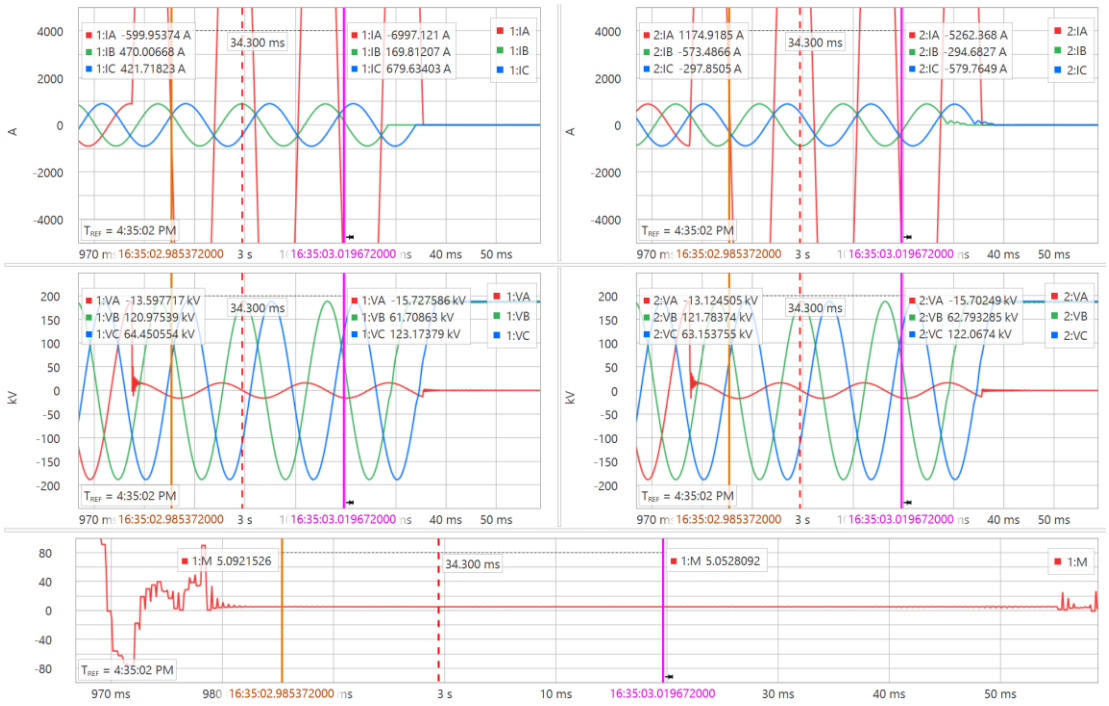

Figure 5.6 AG TOW Fault at 50% - Terminal Voltages and Current, Calculated Fault Location m

Calculations
A=COMPLEX_MA(1,120)
I2.A = (IA.Phasor+A*A*IB.Phasor+ A*IC.Phasor)/3
V2.A = (VA.Phasor+A*A*VB.Phasor+ A*VC.Phasor)/3
m1=1:V2.A-2:V2.A
m2=COMPLEX_MA(Z1MAG.Set,Z1ANG.Set)*(1:I2.A+2:I2.A)
m3=2:I2.A
m4=1:I2.A+2:I2.A
m=REAL(m1/m2+m3/m4)*LL.Set

Figure 5.7 SynchroWAVe Calculations for I2, V2, and DE-Z FL m

Comparing the plots for an AG fault at 50% of the line to the same plots for a similar fault at 25% of the line shown in Figure 5.8 and 5.9, a clear distinction in the delta between the negative-sequence magnitudes of the two terminals demonstrates the effect of the fault location on DE-Z calculations. The V2 magnitudes and angles matching closely lead to the first half of equation (1.7) canceling out, leading to a smaller impact by Z2, in the imbalanced fault shown. The relatively equal magnitude and angle of the negative-

sequence currents from each terminal will result in a ratio of 0.5. Thus, a more accurate estimation is achieved by the DE-Z method when the fault is near the middle of the line.

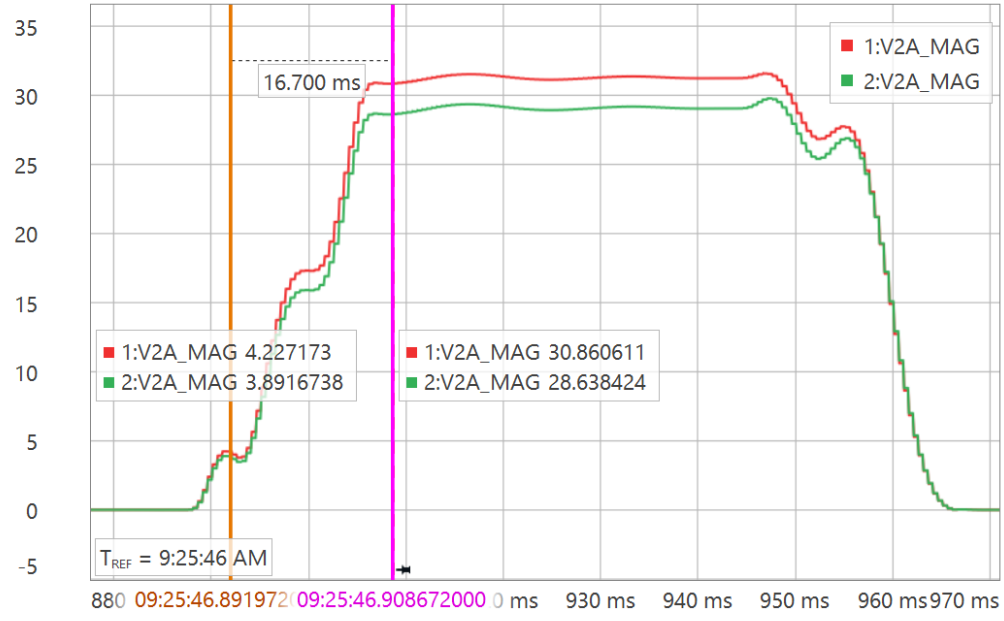

(a)

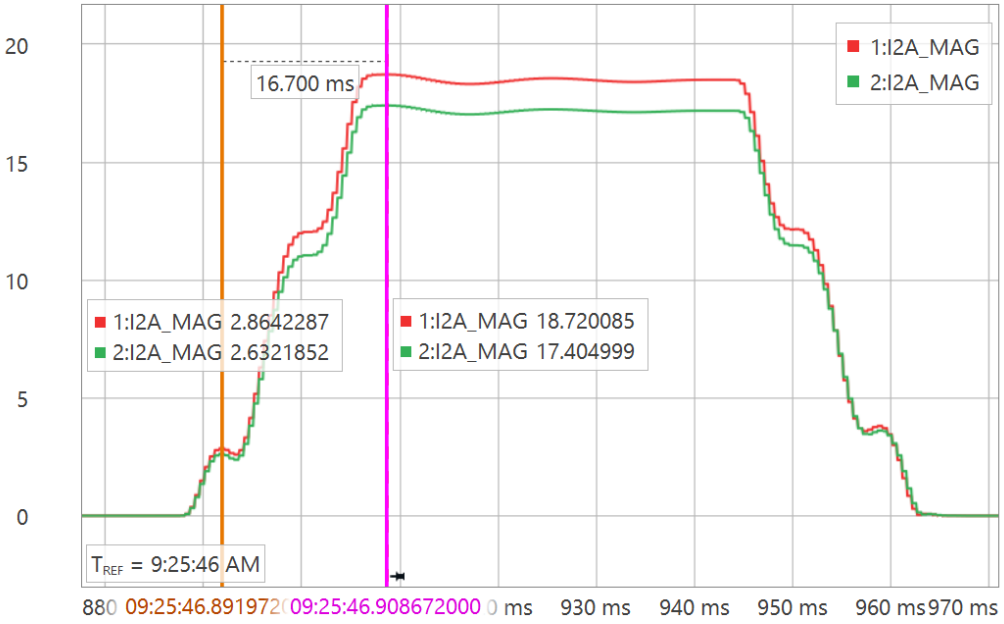

(b)

Figure 5.8 AG TOW Fault at 25% - Negative-Sequence (a) Voltage and (b) Current Magnitudes

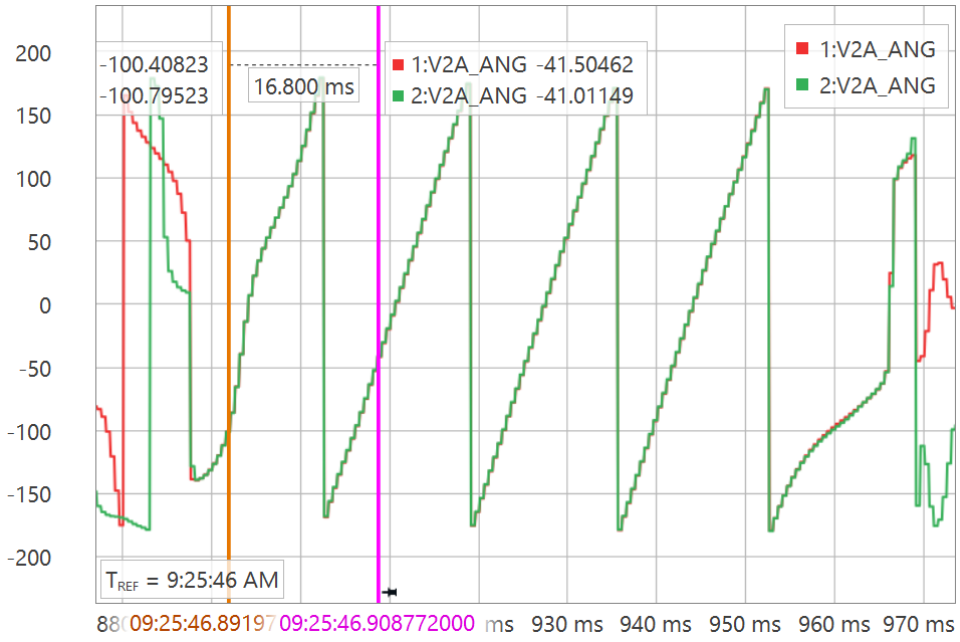

(a)

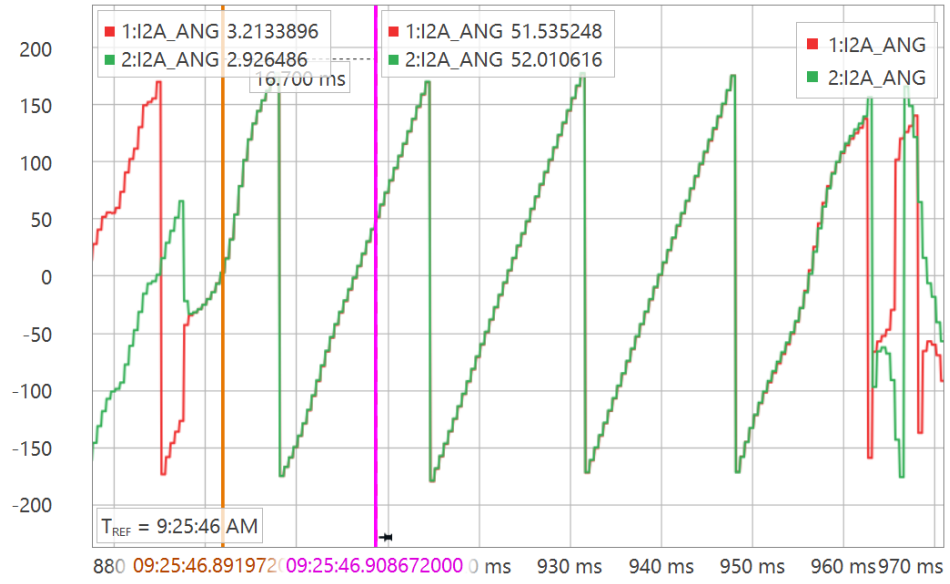

(b)

Figure 5.9 AG TOW Fault at 25% - Negative-Sequence (a) Voltage and (b) Current Angles

The point-on-wave where the fault occurred has its greatest impact on the detectability of the first traveling-wave where if the energy of the first wave is not sufficient for detection by the relay algorithm, it may be missed. However, it has no meaningful

impact on the accuracy of the DE-TW method when the waves are detected. This can be seen in Figures 5.10 through 5.12 for the "Middle of the Waveform" compared to the figures for "Top of the Waveform".

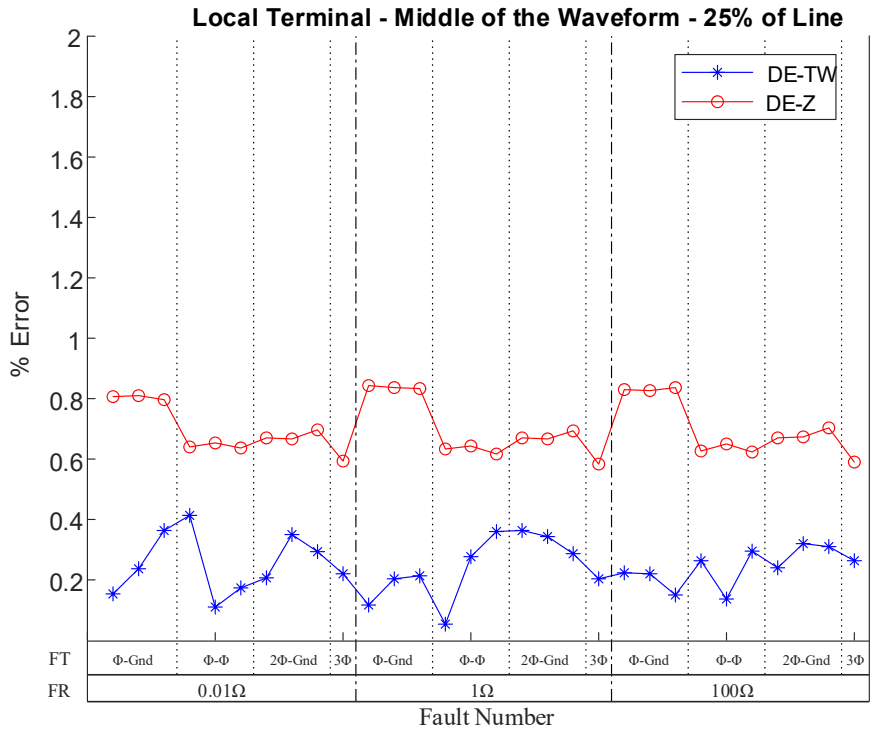

Figure 5.10 FL Error Comparison for MOW with Fault at 25% of Line

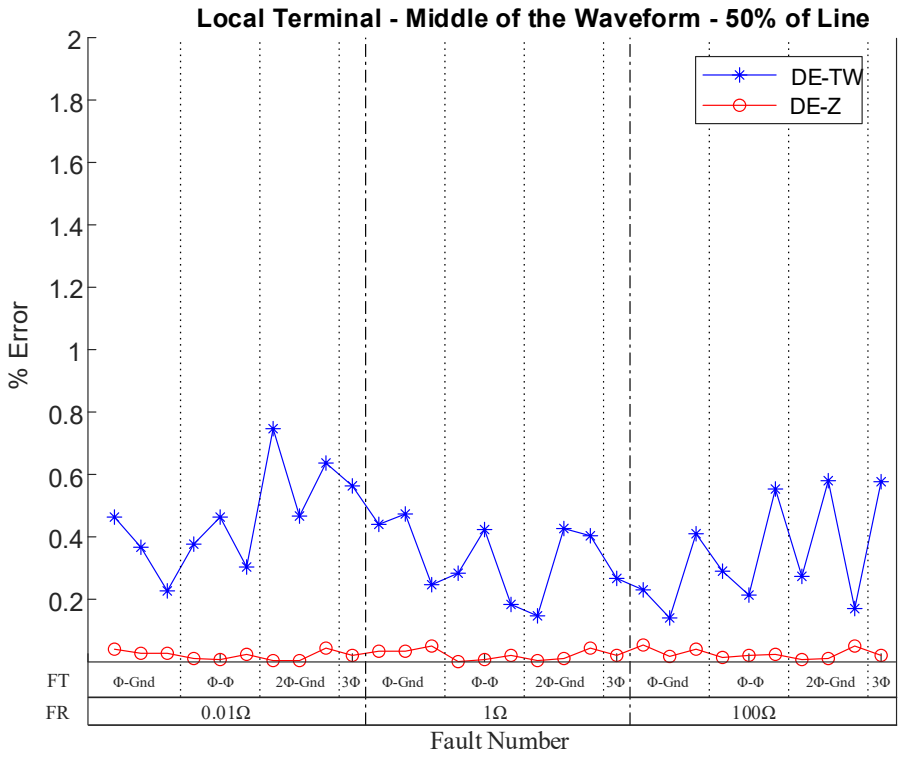

Figure 5.11 FL Error Comparison for MOW with Fault at 50% of Line

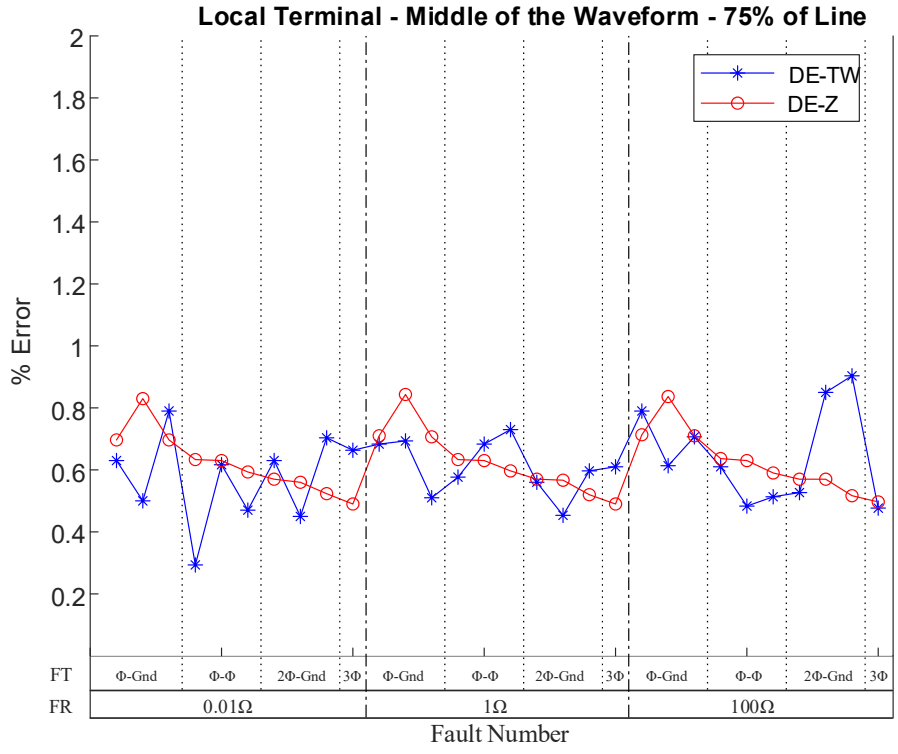

Figure 5.12 FL Error Comparison for MOW with Fault at 75% of Line

It was observed that the first TW of phase-phase faults were most prone to being missed when the fault occurred in the middle of the wave. This outcome can be explained by the fact that at such points the TW beta currents which are used for phase-phase detections can be close to each other in magnitude for the two affected phases. Thus, per equation (5.1) used for beta current/voltage calculations [10], as a result of the close value of the phase currents, the beta current magnitudes may be insufficient for detection.

$$TWI(\Phi 1)(\Phi 2).beta = \frac{TWI(\Phi 1) - TWI(\Phi 2)}{\sqrt{3}} \tag{5.1}$$

An example of the TW beta current for a phase-phase fault at the top of the waveform, Figure 5.13, compared to one in the middle of the waveform, Figure 5.14, shows the noticeable delta in the first TW magnitudes. Analyzing these magnitude differences demonstrates the effect the fault POW on the first TW energy which could cause the energy to be insufficient for detection in some cases. In these figures, the red lines are the TW beta currents from the local terminal (1:TWIAB.beat) and the green lines are from the remote terminal (2:TWIAB.beta). Therefore, the time delta between the first TWs from each terminal can be used to calculate the DE-TW FL which in this case results in the expected 25% of the line, around 2.5 km given a TWLTP of 80.24μs.

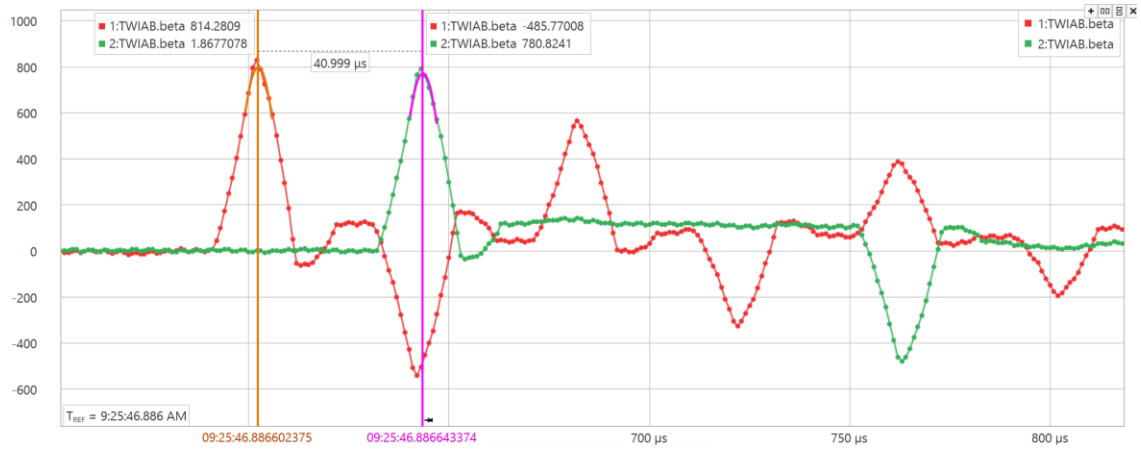

Figure 5.13 TW Beta Currents for AB Fault at Top-of-the-Waveform

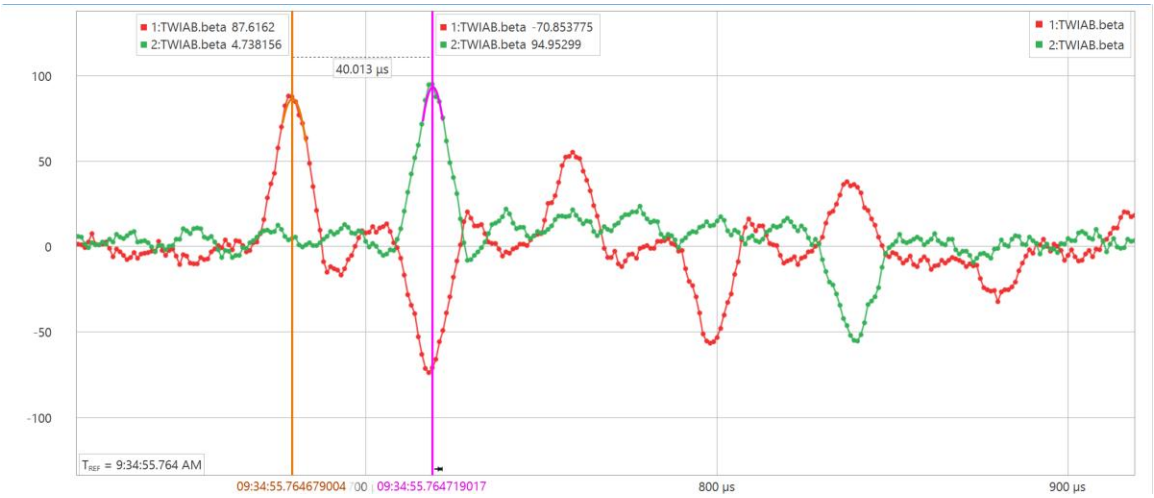

Figure 5.14 TW Beta Currents for AB Fault at Middle-of-the-Waveform

In the zero-crossing cases, the fault types most prone to being missed are the phase-ground faults. This is due to the lower energy of the first TW on any single phase to ground fault when at or near the zero-crossing point. However, faults occurring at such instances can be extremely rare. Therefore, they are not found to be a concern.

The fault resistance has no noticeable impact on either the DE-TW or the DE-Z FL method. The only potential impact could be on the magnitude of the first TW for the DE-TW estimation. However, no remarkable impact was observed in any of the cases regarding the frequency of missing TWs. As expected, the accuracies are all together not impacted by the fault resistance.

Table 5.2 shows the average error for all cases shown in the plots. The averages are shown in percentage error and meters of error for a more intuitive understanding of the distances needed to be inspected by line workers to find the exact location of the fault.

Table 5.2 FL Error Averages

Fault Characteristics		**% Error**		**Error (m)**	
Fault Location	**POW**	**DE-TW**	**DE-Z**	**DE-TW**	**DE-Z**
25%	TOW	0.2756	0.6071	27.56	60.71
	MOW	0.2454	0.7007	24.54	70.07
50%	TOW	0.4297	0.0211	42.97	2.11
	MOW	0.3781	0.0226	37.81	2.26
75%	TOW	0.6054	0.5679	60.54	56.79
	MOW	0.6106	0.6253	61.06	62.53

5.5.2 Cable Characteristic Effects

Transposing the cable cores impacts the line positive-sequence impedance through balancing the mutual coupling between the conductors and the sheaths. This helps with reducing the circulating current in the sheath layers. Transposition of the cable cores offers an improvement on reducing the error in FL estimations of the DE-Z method as evident in Figures 5.15 to 5.17. Depending on the specific considerations for a cable transmission line project, such as cost and practicality, transposing the cables may not be necessary, especially for shorter lines as it does not seem to offer any significant advantages. For longer cables, however, due to the larger electromagnetic coupling effects and the greater impact of FL estimation errors in terms of the actual distances needed to be inspected, advantages of cable transposition may become more considerable.

Cable transposition helps with making the accuracy of the DE-TW method uniform across all fault locations given that transposition for the most part cancels out all mutual electromagnetic coupling between the phases and creates a more homogenous impedance profile. The TWLPT should be recalculated depending on whether the cables transposed or not as it does lead to non-negligible impacts on the wave propagation velocity through the cable, especially for longer cables as the differences compound.

The results for transposed versus untransposed cables when the fault is applied in the middle of the wave were found to follow a similar pattern as described before. Since no new findings were drawn from those results, they are included at the end of the analysis. As previously discussed, the only notable effect of MOW faults is on the DE-TW method detecting the first TW depending on whether it has sufficient energy under phase-phase fault conditions. However, when manually checked and calculated using the TW beta voltages and currents in the Bewley diagram, quite accurate fault locations can be found.

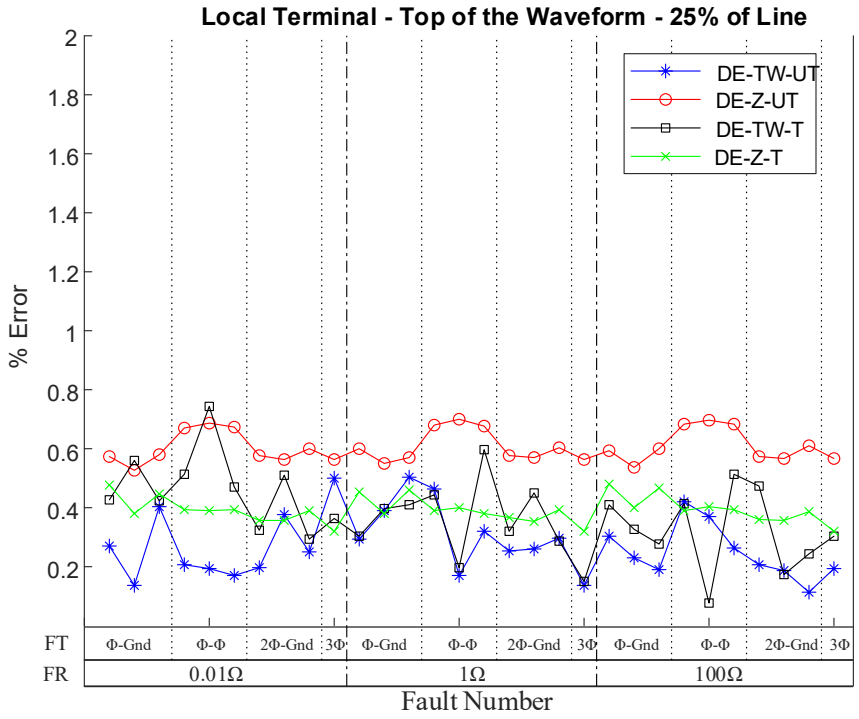

Figure 5.15 FL Error Comparison for TOW with Fault at 25% of Line

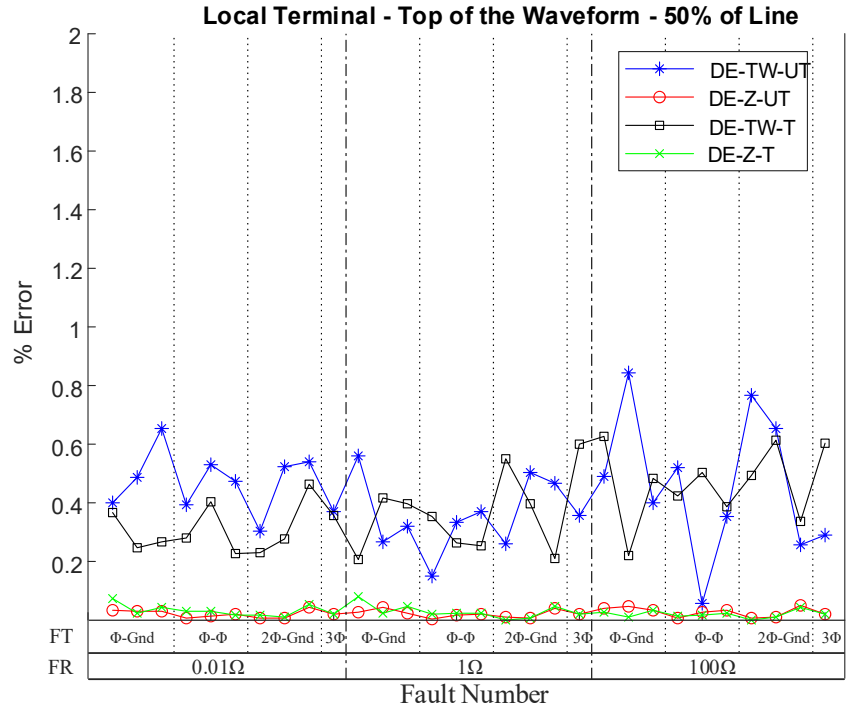

Figure 5.16 FL Error Comparison for TOW with Fault at 50% of Line

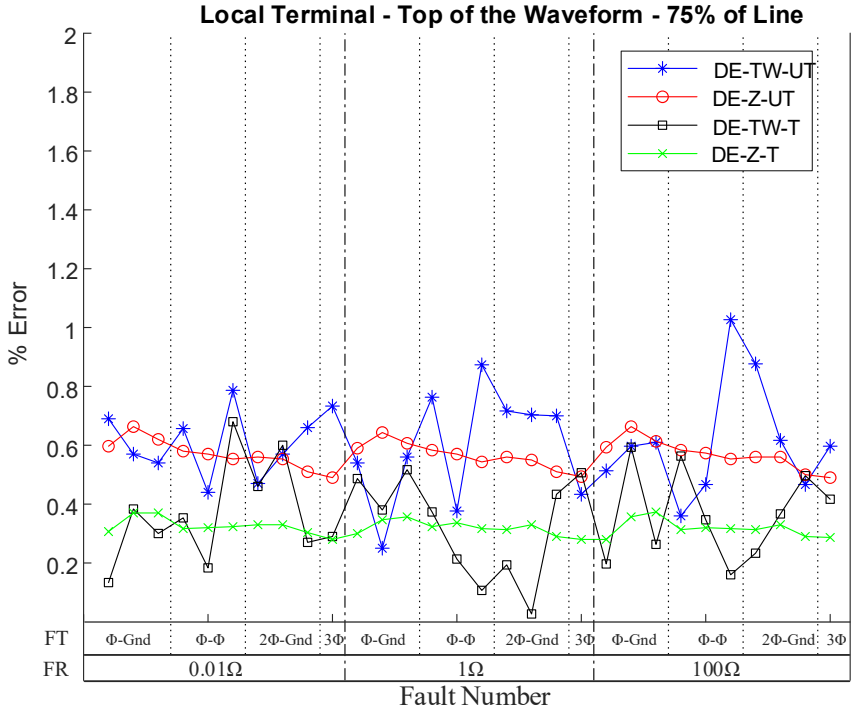

Figure 5.17 FL Error Comparison for TOW with Fault at 75% of Line

Table 5.3 shows the average error for all transposed versus untransposed cases.

Table 5.3 FL Error Averages for Transposed and Untransposed Cables

Cable Characteristics	**Fault Characteristics**		**% Error**		**Error (m)**	
Untransposed	**Fault Location**	**POW**	**DE-TW**	**DE-Z**	**DE-TW**	**DE-Z**
	25%	**TOW**	0.2756	0.6071	27.56	60.71
		MOW	0.2454	0.7007	24.54	70.07
	50%	**TOW**	0.4297	0.0211	42.97	2.11
		MOW	0.3781	0.0226	37.81	2.26
	75%	**TOW**	0.6054	0.5679	60.54	56.79
		MOW	0.6106	0.6253	61.06	62.53
Transposed	**Fault Location**	**POW**	**DE-TW**	**DE-Z**	**DE-TW**	**DE-Z**
	25%	**TOW**	0.3797	0.3919	37.97	39.19
		MOW	0.398	0.4714	39.8	47.14
	50%	**TOW**	0.3818	0.0268	38.18	2.68
		MOW	0.4029	0.026	40.29	2.6
	75%	**TOW**	0.3509	0.3208	35.09	32.08
		MOW	0.3886	0.3888	38.86	38.88

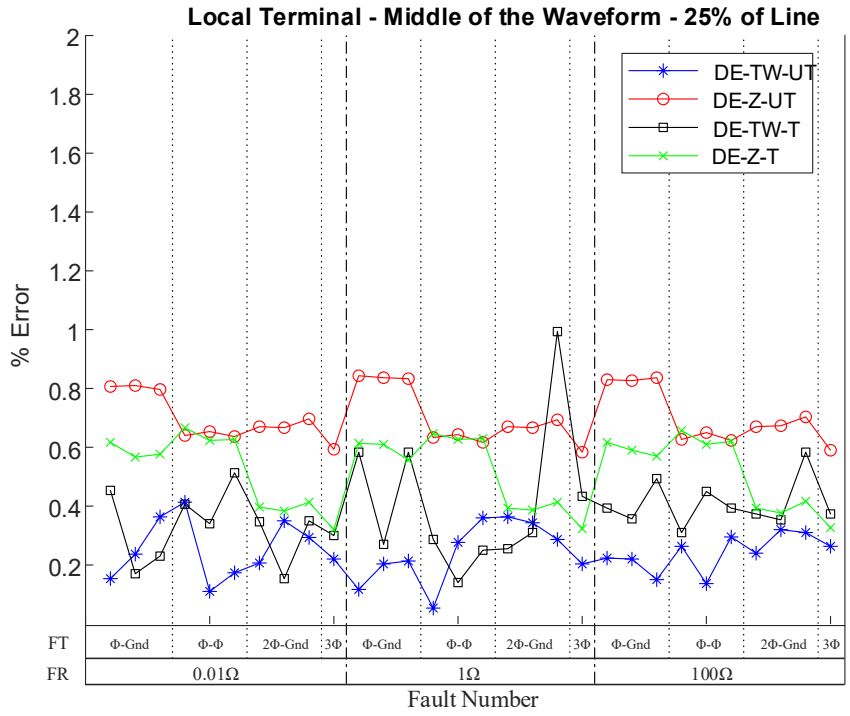

Figure 5.18 FL Error Comparison for MOW with Fault at 25% of Line

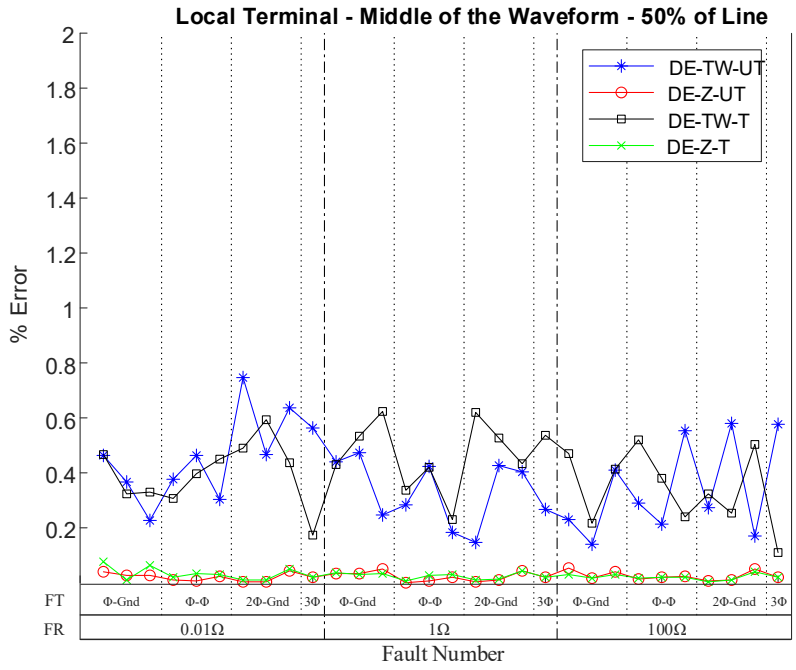

Figure 5.19 FL Error Comparison for MOW with Fault at 50% of Line

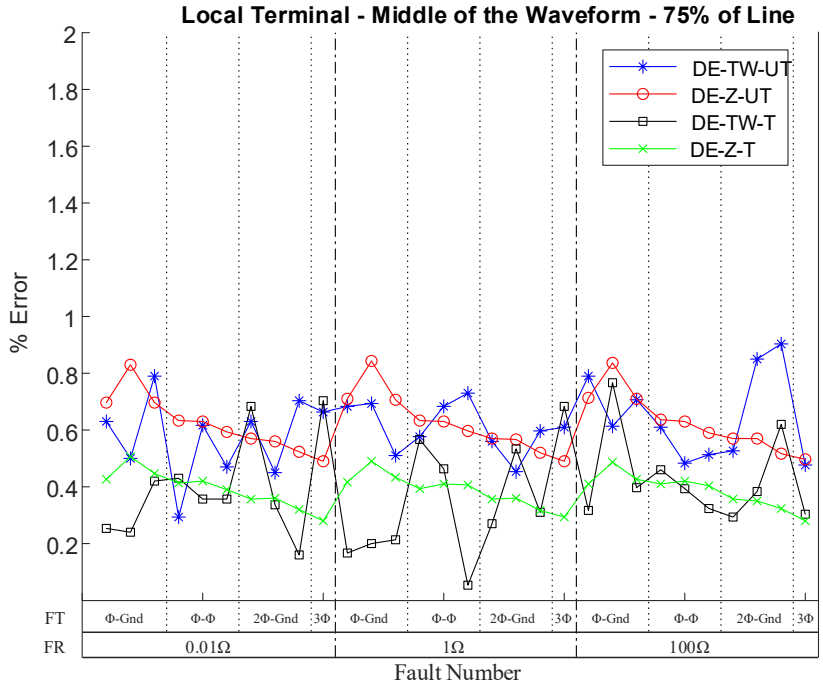

Figure 5.20 FL Error Comparison for MOW with Fault at 75% of Line

CHAPTER 6: CONCLUSION

6.1 Research Overview

The experiences and lessons learned from the tests performed in the course of these studies can be used in setting up HIL experiments for testing and validation of relay settings commissioned in power systems with UG cables. Using RTDS and RSCAD, a power system model was developed incorporating the 10 km long cable model used for testing. The RTDS-based HIL setup sent real-time signals to the T401L relay which performed the fault location estimations that were processed as the results of these studies. Performing such real-time tests on a relay in an open or closed loop setup can be crucial before commissioning major projects in order to make sure of the integrity of the settings and minimize mis-operations. All information about the setup can be found in Chapter 4 with complementary details in the corresponding appendix sections. As part of these setups, the methods for determining the necessary settings for the T401L's DE-TW and DE-Z FL methods were also discussed.

All practical results from the testing done on the T401L for both fault locating methods were analyzed and included in Chapter 5. The criteria that were used to test the FL accuracy of each method were grouped into the fault characteristics and cable characteristics, detailed in Table 5.1, whose theoretical concepts were expanded on in the introductory chapters. The theory behind DE-TW and DE-Z was also explained in the first chapter, which forms the basis for the analysis of each FL method based on the results. All results were analyzed per the line-length-standardized percentage error.

6.2 Research Contributions Summary

Overall, both FL methods proved to be very accurate under all fault conditions even with the cable being untransposed. The symmetrical nature and relative simplicity of the power system in which the tests were conducted has to be considered. The aim of these tests is to one: provide a practical set of lessons and be a guide for setting up similar HIL tests for further testing with more complex cases; and two: share findings and analysis of the results for engineers implementing fault locating relays into the power grid.

Trust in the accuracy of these FL relays and considerations for their dependability under different conditions are crucial. Therefore, similar tests can be conducted by incorporating the FL relay into HIL test with a utility's simulated power system in order to ensure of the integrity of the fault locating design and relay settings based on the specific idiosyncrasies of the power system they are implemented in.

The accuracy of FL estimation is primarily influenced by fault and cable characteristics, notably the fault location, fault point-on-wave, fault type, and cable core transposition. The analysis focuses exclusively on cross-bonded cables in trefoil formation to isolate these effects. The results show a clear trend where the DE-TW method's accuracy is less impacted by the location of the fault, while the DE-Z method performs better for faults near the middle of the line in a homogenous system with evenly distributed line impedances and similar SIRs on both terminals. This behavior is evident when comparing results for faults at 25% and 75% versus 50% of the line length. When faults occur near the middle of the line, the negative-sequence voltages and currents at both terminals closely match in magnitude and angle, causing partial cancellation in the DE-Z equations and yielding a current ratio of about 0.5. This leads to improved DE-Z accuracy for mid-line

faults when the two buses have similar voltages, dynamics, and SIRs. Comparatively, the DE-TW method is more consistently accurate for all fault locations especially when the cable cores are transposed.

The fault point-on-wave mainly affects the detectability of the first Traveling-Wave rather than the accuracy of DE-TW once detection occurs. The first TW energy may be insufficiently low in magnitude, particularly for phase-phase fault near the middle of the wave and phase-ground faults near the zero-crossing point, to where it could be missed by the algorithm. Though such cases are rare and therefore not considered a major concern given the extreme rarity of phase-phase faults in underground cables and of faults occurring in the vicinity of the zero-crossing point. In phase-phase faults occurring near the middle of the waveform, the smaller magnitude of the TW beta voltage and current magnitudes is caused by the values of the voltage and current phasors of the affected phases being very close to each other.

Fault resistance was found to have no meaningful impact on the accuracy of either DE-TW or DE-Z methods. Although higher resistance could theoretically reduce traveling-wave magnitude, no notable increase in missed detections or accuracy degradation was observed across the analyzed cases.

Cable transposition introduces improvements to the DE-Z FL estimation method which would be useful for long cables as the compounded errors of the untransposed cable versus the transposed cable could add to more noticeable fault location errors. The DE-TW method also benefits from the more homogenous cable impedances, which leads to the accuracies matching more closely regardless of the fault location and POW. The TWLPT setting value needs to be recalculated based on the configuration of the cable. This is

especially important for longer cables as the wave propagation velocity is impacted more by the transposition as the cable length increases.

To ensure that the fault location is identified with the greatest accuracy, it is best practice to use the double-ended fault locating methods as they have access to more data and therefore are much more accurate than their single-ended counterparts. As it has been observed from real-world applications [3], and supported by the findings from the test conducted through this research, the DE-TW method's use of high-frequency traveling-waves makes it much more robust against impedance discontinuities and other cable characteristics such as greater shunt capacitances. The DE-TW method only needs one data point from each terminal, that being the first TW arrival time. Therefore, it is extremely fast and does is not impacted by fast operating breakers that could open in once cycle or less which can impact the accuracy of the DE-Z method given that it averages a certain number of points after the fault for its fault locating calculations. Thus, as it is common practice when fault locating relays are available are both terminals of a line/cable, to use DE-TW method as the primary FL method and the DE-Z method as backup. More advanced algorithms and practices and be developed based on the specific characteristics of the power system in question. For instance, provided that the necessary system symmetry is present, a design could be implemented to use the DE-TW method primarily, unless both methods determine the fault to be close to the middle of the line, wherein the DE-Z could be primarily used given its higher observed accuracy at the line midpoint.

6.3 Future Work and Vision

The test will be expanded to include more testing criteria regarding more complex power systems, fault conditions, and cable characteristics. Such complexities include:

- Longer cables, particularly the effects on the line impedances used in DE-Z and the accuracy of the TWLPT calculations used in the DE-TW method.
- Hybrid transmission lines with overhead and underground sections, useful for blocking reclosing on faults in the UG section(s).
- Evolving faults, especially the impacts on DE-TW given the addition of new traveling-waves coming in soon after the initial first TW.
- Performing tests on more fault locations to 1. Thoroughly validate the observations seen on the differences between the accuracies of the two methods based on whether the fault is close to the terminals or near the middle of the line 2. Test the effects of other fault locations on each method's accuracy, especially as the faults get closer to the terminals.
- Testing a wider range of fault POW and comparing the results with the original findings.
- Adding more complexities to the power system, such as parallel lines and transformers.
- Running studies and comparing results with similar real-world scenarios would provide an excellent reference with which the FL methods could be tested.

REFERENCES

[1] D. A. Tziouvaras, "Protection of High-Voltage AC Cables," 2006 Power Systems Conference: Advanced Metering, Protection, Control, Communication, and Distributed Resources, Clemson, SC, USA, 2006, pp. 316-328.

[2] D. Bucco et al., "Protection challenges for North America's first combined cable/overhead double-circuit 500 kV transmission line with mutual coupling," 2017 70th Annual Conference for Protective Relay Engineers (CPRE), College Station, TX, USA, 2017, pp. 1-15.

[3] O. N. Ogbogu and I. C. Amadi, "Review on Enhancement of Electric Power Transmission using Underground Cabling," International Journal for Research in Applied Science and Engineering Technology, vol. 7, no. 12, pp. 519–524, Dec. 2019.

[4] D. A. Tziouvaras, "Calculating Intermediate Faults in Underground Cables," 2012. [Online] Available: https://cdn.selinc.com/assets/Literature/Publications/Technical%20Papers/6563_CalculatingIntermediate_DT_20120904_Web2.pdf?v=20151125-093033

[5] Y. Xue, D. Finney, and B. Le, "Charging Current in Long Lines and High-Voltage Cables - Protection Application Considerations," 2012. [Online] Available: https://cms-cdn.selinc.com/assets/Literature/Publications/Technical%20Papers/6574_ChargingCurrent_DF_20120914_Web2.pdf?v=20151125-000900 [6] Impedance-Based Fault Location Experience

[7] A. Shrestha and S. K. Mutha, "New multi-ended fault-locating method utilizing incremental sequence quantities," 17th International Conference on Developments in Power System Protection (DPSP 2024), Manchester, UK, 2024, pp. 387-393.

[8] T. Banerjee, Z. Miao and L. Fan, "Traveling Wave Based Fault Location Methods: Review and Demonstration," 2023 North American Power Symposium (NAPS), Asheville, NC, USA, 2023, pp. 1-6.

[9] B. Kasztenny, A. Guzmán, N. Fischer, M. Mynam, and D. Taylor, "Practical Setting Considerations for Protective Relays That Use Incremental Quantities and Traveling Waves," 2016. [Online] Available: https://selinc.com/api/download/117051/

[10] SEL-T401L Ultra-High-Speed Line Relay Instruction Manual, 20251120 ed. SEL, Pullman., WA, USA, 2025. [Online]. Available: https://selinc.com/products/T401L/docs/

[11] C. L. Bak and F. Faria da Silva, "High Voltage AC underground cable systems for power transmission – A review of the Danish experience: Part 2," Electric Power Systems Research, vol. 140, pp. 995–1004, Nov. 2016.

[12] RTDS Cable Constants Manual, March 2015 rev01. RTDS Technologies, Winnipeg, MB, Canada, 2015.

[13] C. L. Bak and F. Faria da Silva, "High voltage AC underground cable systems for power transmission – A review of the Danish experience, part 1," Electric Power Systems Research, vol. 140, pp. 984–994, Nov. 2016.

[14] "IEEE Guide for the Application of Sheath-Bonding Methods for Single-Conductor Cables and the Calculation of Induced Voltages and Currents in Cable Sheaths," in ANSI/IEEE Std 575-1988, vol., no., pp.0_1-, 1987.

[15] "IEEE Guide for Determining Fault Location on AC Transmission and Distribution Lines," in IEEE Std C37.114-2014 (Revision of IEEE Std C37.114-2004), vol., no., pp.1-76, 30 Jan. 2015.

[16] J. C. Das, “Unsymmetrical Fault Calculations,” in Power System Analysis : Short-Circuit Load Flow and Harmonics, Second Edition, H. L. Williams and M. H. Rashid, Eds., CPC Press Taylor & Francis Group, LLC, 2012.

[17] N. M. Khoa, M. V. Cuong, H. Q. Cuong, and N. T. T. Hieu, “Performance Comparison of Impedance-Based Fault Location Methods for Transmission Line,” International Journal of Electrical and Electronic Engineering & Telecommunications, pp. 234–241, 2022.

[18] S. S. B. Azevedo, R. L. S. França, J. T. L. S. Campos, and F. B. Costa, “Comprehensive Analysis of the Fault Inception Angle Influence in Fault-Induced Traveling Waves,” Electric Power Systems Research, vol. 195, p. 107161, Jun. 2021.

[19] RTDS Hardware Manual, 20230531. RTDS Technologies, Winnipeg, MB, Canada, 2015.

[20] "IEEE Guide for Protective Relay Applications to Transmission Lines," in IEEE Std C37.113-2015 (Revision of IEEE Std C37.113-1999), vol., no., pp.1-141, 30 June 2016.

[21] A. Makki, M. Rothweiler, R. Orndorff, and J. B. Starling, “An Investigation of the Energy Consumption by Information Technology Equipments,” International Journal of Computer Science and Information Technology, vol. 5, no. 2, pp. 33–40, May 2013.

APPENDIX A: CABLE PARAMETERS

A.1 Cable Parameters

The following are the physical and electrical parameters of the cable as defined in the "Protection of High-Voltage AC Cables" paper [1]. All resistivity values are defined 20°C.

- Cable Type: 1,200 mm2 XLPE with copper conductor core
- Cable Operating Voltage: 230 kV
- Cable Length: 10 km
- Conductor Radius: 2.15 cm
- Conductor Resistivity: 1.72 E-08 Ωm
- Insulation Radius: 4.52 cm
- Insulation Relative Permittivity: 2.5
- Sheath Radius: 4.98 cm
- Sheath Resistivity: 2.14 E-07 Ωm
- Polyvinyl Chloride (PVC) radius: 5.38 cm
- PVC Permittivity: 8.0
- Earth Resistivity: 100.0 Ωm

A.2 Cable Parameters in RSCAD Cable Editor

Below are the cable parameters as entered in RSCDAD's Cable Editor. Please note that this is the cable model for one of the four cable sections used in the power system model, thus the cable length is a quarter of the total length, 2.5 km. The parameters are the same for all cable sections.

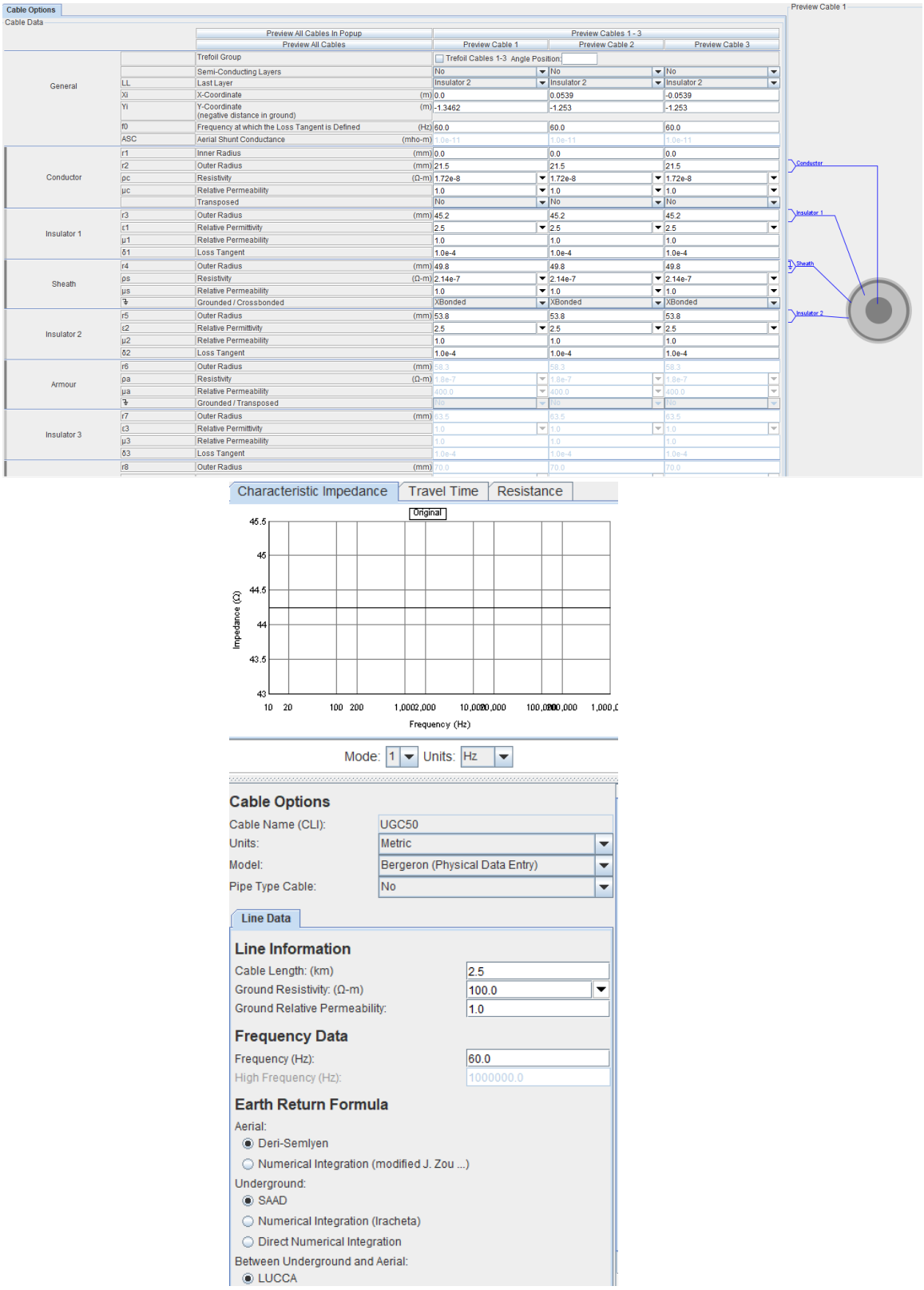

Figure A.1 RSCAD Cable Parameters (a) Physical Characteristic Inputs (b) Cable Options

A.3 Cable Sequence Impedances

The positive- and zero-sequence impedances of each cable section can be found in the ".map" file generated by the RSCAD model once the power system model is compiled. These line sequence impedances are very useful for power system studies and configuring the relay settings. Given that all cable sections are of equal length, these parameters are the same for all sections.

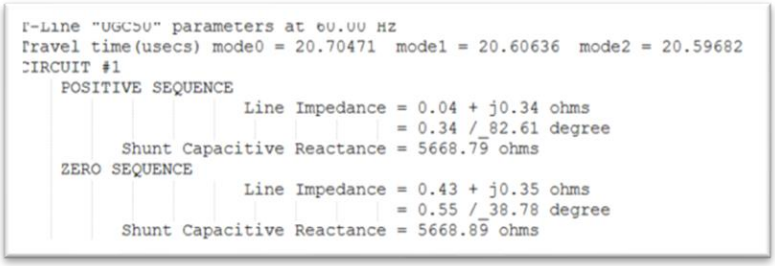

Figure A.2 Cable Sequence-Impedance Data from the .map File [12]

Additional data about the impedance profile of each cable section can be found in the "_out" files. This information includes the positive- and zero-sequence resistance, reactance, and susceptance. A very useful piece of information is also the minimum time delay for the model. An example is shown below.

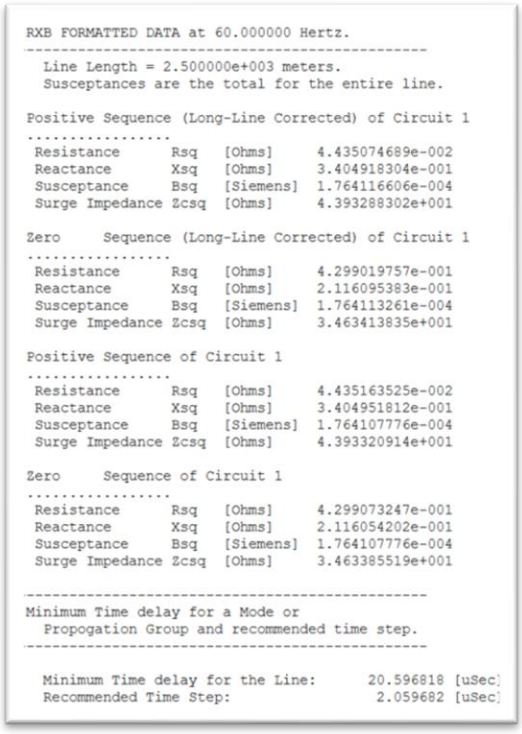

```
RXB FORMATTED DATA at 60.000000 Hertz.
-------------------------------------------------
  Line Length = 2.500000e+003 meters.
  Susceptances are the total for the entire line.

Positive Sequence (Long-Line Corrected) of Circuit 1
..................
 Resistance       Rsq   [Ohms]      4.435074689e-002
 Reactance        Xsq   [Ohms]      3.404918304e-001
 Susceptance      Bsq   [Siemens]   1.764116606e-004
 Surge Impedance Zcsq   [Ohms]      4.393288302e+001

Zero     Sequence (Long-Line Corrected) of Circuit 1
..................
 Resistance       Rsq   [Ohms]      4.299019757e-001
 Reactance        Xsq   [Ohms]      2.116095383e-001
 Susceptance      Bsq   [Siemens]   1.764113261e-004
 Surge Impedance Zcsq   [Ohms]      3.463413835e+001

Positive Sequence of Circuit 1
..................
 Resistance       Rsq   [Ohms]      4.435163525e-002
 Reactance        Xsq   [Ohms]      3.404951812e-001
 Susceptance      Bsq   [Siemens]   1.764107776e-004
 Surge Impedance Zcsq   [Ohms]      4.393320914e+001

Zero     Sequence of Circuit 1
..................
 Resistance       Rsq   [Ohms]      4.299073247e-001
 Reactance        Xsq   [Ohms]      2.116054202e-001
 Susceptance      Bsq   [Siemens]   1.764107776e-004
 Surge Impedance Zcsq   [Ohms]      3.463385519e+001

-------------------------------------------------
Minimum Time delay for a Mode or
  Propogation Group and recommended time step.
-------------------------------------------------

  Minimum Time delay for the Line:      20.596818 [uSec]
  Recommended Time Step:                 2.059682 [uSec]
```

Figure A.3 Cable Sequence-Impedance Data from the _out File [12]

APPENDIX B: RSCAD POWER SYSTEM MODEL

The two-bus system designed in RSCAD has a 230 kV source connected through an UG cable transmission line is divided into four equal sections. An example of the fault block with the relevant information that is changed by the automated script is also shown.

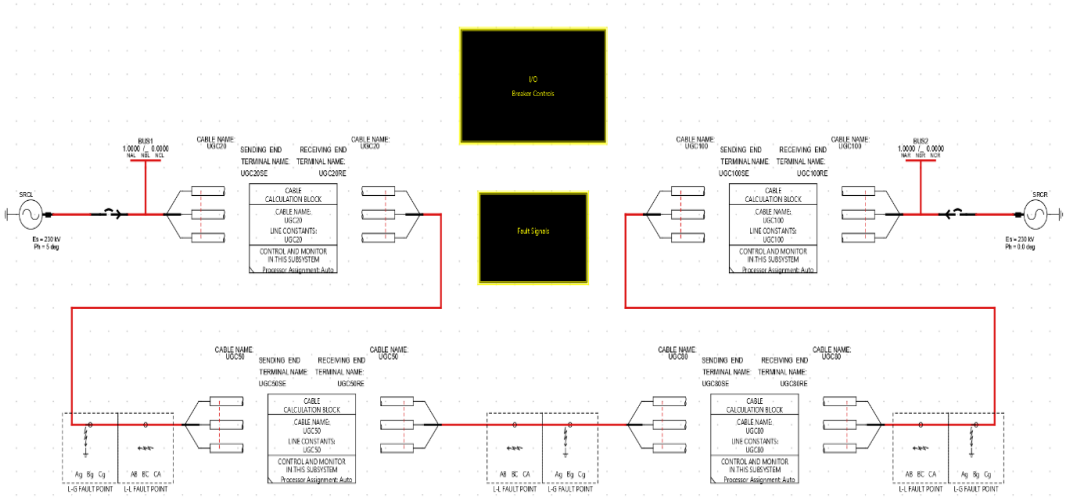

Figure B.1 Two-Source Power System Designed in RSCAD

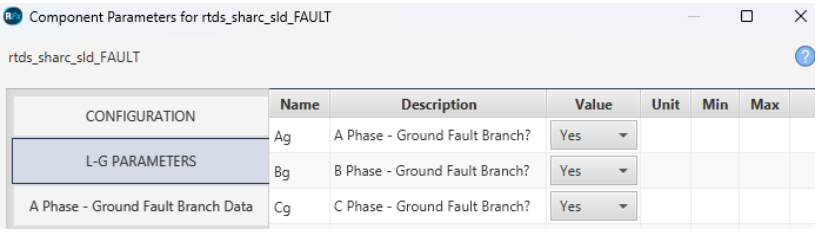

Figure B.2 Line-Ground Fault Block Parameters Example

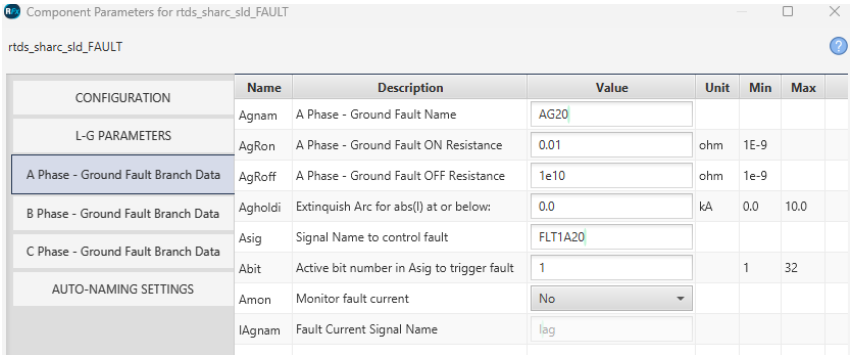

Figure B.3 AG Fault Parameters Example

APPENDIX C: HIL-RTDS/RSCAD CONFIGURATION

C.1 RSCAD-HIL Setup

In RSCAD, the metered voltages and currents from each terminal getting transformed into the secondary values of the relay, given that the specialized T401L used in this experiment take low-energy inputs that bypass the internal CTs and PTs of the relay. Then these signals are inputted to the GTAO to be injected into the relays.

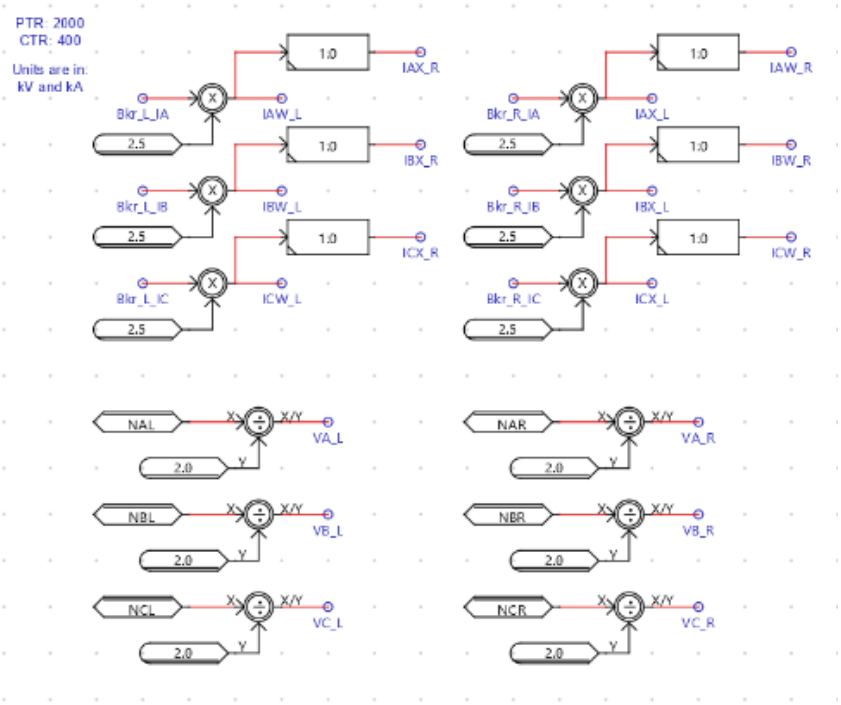

Figure C.1 CT and PT Conversions for Low Energy Input Setup

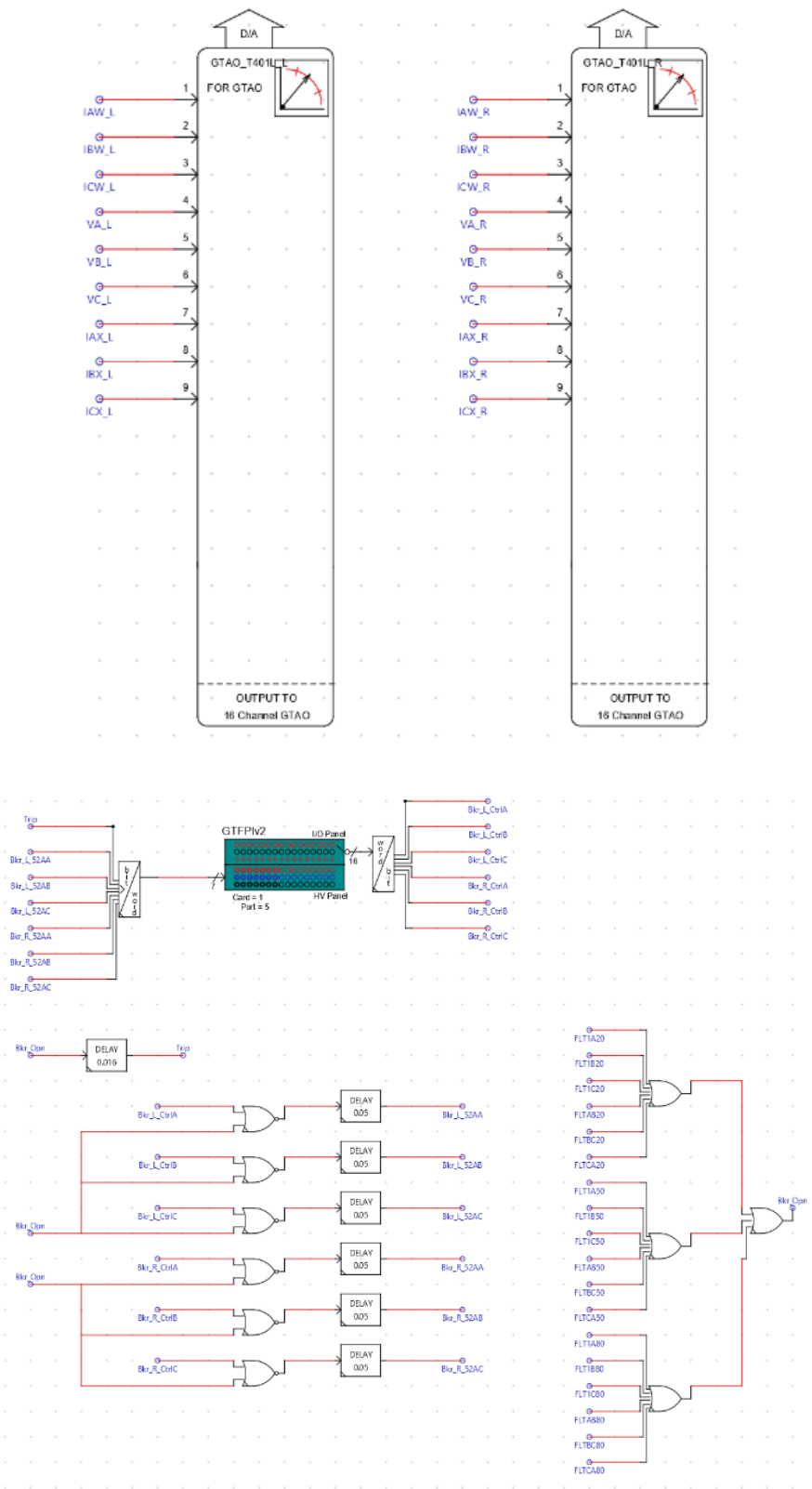

Figure C.2 GTAO and GTFPI Connections

The T401L takes in digital signals such as breaker status signals from the GTFPI. In a closed loop system, the relay can also send signals to the RSCAD model such as the Trip and breaker closure signals.

For these tests, the *Trip* signal was sent to the relay's IN101 from the RSCAD model to standardize the tripping time of the relays for all cases. For protection testing, the trip signal would typically come from the relay to open the breakers.

C.2 Automated Script

The automated script calls on each object within the RSCAD model such as the line-ground fault block shown below, based on its unique *Object ID*. This enables the script to change values, control, and read from all objects in either the *Draft* or the *Runtime* panels.

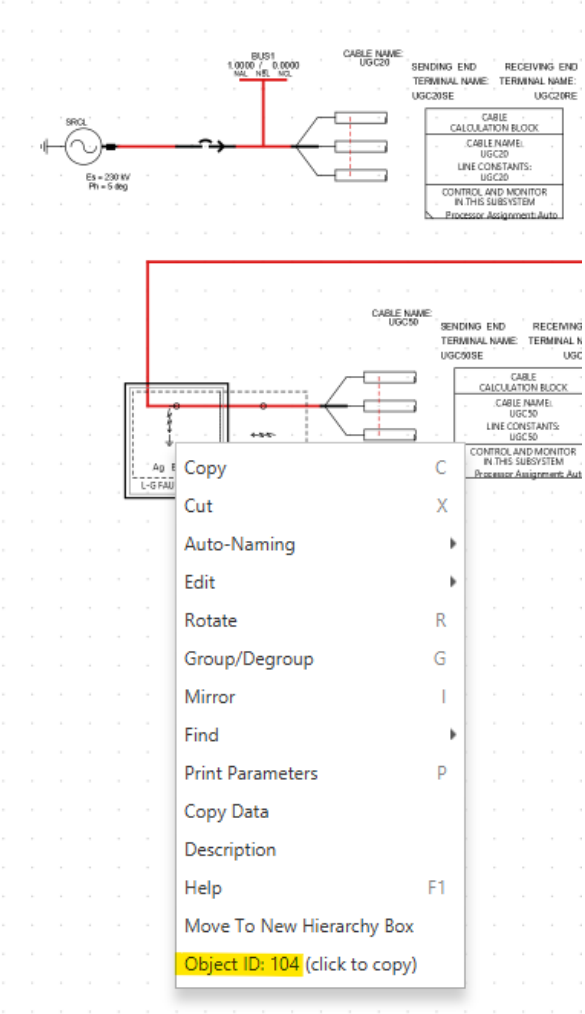

Figure C.3 Retrieving Object ID in RSCAD Example

A python script was used, with the use of the proper libraries calls such as the *rtds.rscadfx*, to automate the testing process through running batches of test cases with different fault conditions and cable characteristics. The script changed the values of objects in the *Draft* page of the RSCAD model such as the fault objects and controlled signals in the *Runtime* page such as triggering faults. The main script, also called on other scripts to perform tasks on the relay such as clearing the event history, sending settings, and collecting event reports. These event reports are then processed and put into a table

format which is saved as a .CSV file to be processed by a MATLAB script to plot the final results in the desired format.

```
import rtds.rscadfx
from pathlib import Path
from datetime import datetime
import os
import csv
import shutil
import time
from Clear_Relay import Clear_Relay
from Collect_Reports import FTPcollect
from Send_Initial_Settings import Send_Initial_Settings
from HDR_parser import HDR_parser

now = datetime.now()
start_time = now.strftime("%H:%M:%S")
print("Start Time =", start_time)

flt_25 = 1
flt_50 = 1
flt_75 = 1

t4011_l_ip = '###'
t4011_r_ip = '###'

col_MHR = 0
HDR_only = 1

model_dir = r"C:..."

# Pre-defined Testing Parameters
load_flow_angle = [5]#,10,-10] # Initial Phase Angle of the Local Bus Generator
fault_resistances = [0.01,1,100]
POW_val = [90, 135 180]
fault_triggers_25 = [309,309,309,310,310,310,311,311,311,
313,313,313,314,314,314,315,315,315,
1282,1282,1282,1283,1283,1283,1284,1284,1284, 1324,1324,1324]
```

```
fault_triggers_50 = [317,317,317,318,318,318,319,319,319,
325,325,325,326,326,326,327,327,327,
1286,1286,1286,1287,1287,1287,1288,1288,1288, 1326,1326,1326]
fault_triggers_75 = [321,321,321,322,322,322,323,323,323,
329,329,329,330,330,330,331,331,331,
1290,1290,1290,1291,1291,1291,1292,1292,1292, 1328,1328,1328]
fault_types = ["AG1","AG2","BG1","BG2","CG1","CG2",
"AB1","AB2","BC1","BC2","CA1","CA2",
"ABG1","ABG2","BCG1","BCG2","CAG1","CAG2", "ABC1","ABC2"]
fault_objects_pg = [104,198,145] # Phase-Gnd Fault Objects
fault_objects_pp = [199,149,200] # Phase-Phase Fault Objects



#clearing out the terminal
os.system('cls')

## Directory setup
# Current Directories
current_dir = Path(os.path.dirname(os.path.abspath(__file__))).parents[0]
py_dir = current_dir

# Comtrades
comtrades_path = os.path.join(current_dir, 'Comtrades')
comtrade_Local = os.path.join(comtrades_path, 'Local_T401L\\')
comtrade_Remote = os.path.join(comtrades_path, 'Remote_T401L\\')

# Results
results_path = os.path.join(current_dir, 'Results')
results_Local = os.path.join(results_path, 'Local_T401L\\')
results_Remote = os.path.join(results_path, 'Remote_T401L\\')
results_csv_dir = os.path.join(current_dir, 'Results.csv')
results_txt_dir = os.path.join(current_dir, 'Results.txt')

# Initial Settings
initial_set_dir = os.path.join(current_dir, 'Initial_Settings\\')
local_t401l_initial_set_dir = os.path.join(initial_set_dir, 'Local_T401L_Settings\\')
local_t401l_set_r = os.path.join(local_t401l_initial_set_dir, 'SET_R.TXT')
local_t401l_set_1 = os.path.join(local_t401l_initial_set_dir, 'SET_1.TXT')
local_t401l_set_P6 = os.path.join(local_t401l_initial_set_dir, 'SET_P6.TXT')
```

```
remote_t401l_initial_set_dir = os.path.join(initial_set_dir, 'Remote_T401L_Settings\\')
remote_t401l_set_r = os.path.join(remote_t401l_initial_set_dir, 'SET_R.TXT')
remote_t401l_set_1 = os.path.join(remote_t401l_initial_set_dir, 'SET_1.TXT')
remote_t401l_set_P6 = os.path.join(remote_t401l_initial_set_dir, 'SET_P6.TXT')


# Analysis Folder
analysisFolder = os.path.join(current_dir,'Analysis\\')

# Set Backup_OldComtrades
Backup_OldComtrades = True
if Backup_OldComtrades:
    # Backup comtrades folder if it exists:
    if os.path.isdir(comtrades_path):
        #Create a backup folder if the backup folder does not exist
        backup_root = os.path.join(current_dir, 'comtrades_old_runs')
        os.makedirs(backup_root, exist_ok = True)

        # Create timestamped folder name
        timestamp = datetime.now().strftime('%d-%m-%Y_%H-%M-%S')
        backup_name = f'comtrades_{timestamp}'
        backup_path = os.path.join(backup_root, backup_name)

        # Move the folder
        shutil.move(comtrades_path, backup_path)
        print(f'Backed up comtrades to: {backup_path}')

## Initial directory
# Check and remove old directories
if os.path.isdir(results_path):
    shutil.rmtree(results_path)

# Recreate clean directories
os.makedirs(results_Local)
os.makedirs(results_Remote)

print(f"\n\n*****Starting Automated Test*****\n")
print("SEL-T401L_L IP: " + t401l_l_ip)
print("SEL-T401L_R IP: " + t401l_r_ip)
```

```
## Clear Relay
print("\n\n**********Clearing Relays**********\n")
Clear_Relay(t401l_l_ip,23, password_level1='OTTER', password_level2='TAIL')
Clear_Relay(t401l_r_ip,23, password_level1='OTTER', password_level2='TAIL')
time.sleep(30)

## Setting up initial settings
initial_settngs_files_local = [local_t401l_set_r,local_t401l_set_1,local_t401l_set_P6]
initial_settngs_files_remote =
[remote_t401l_set_r,remote_t401l_set_1,remote_t401l_set_P6]

# Sending Initial Settings to the Relays
print("\n\n**********Sending Initial Settings to the Local
T401L**********\n")
for settings_files in initial_settngs_files_local:
    Send_Initial_Settings(t401l_l_ip,settings_files)
print("\n\n**********Sending Initial Settings to the Remote
T401L**********\n")
for settngs_files in initial_settngs_files_remote:
    Send_Initial_Settings(t401l_r_ip,settngs_files)

## Run RSCAD Simulation
# Open a connection to RSCAD FX from the script
with rtds.rscadfx.remote_connection() as app:
    # Start Simulation
    simRun = app.open_case(model_dir)
    simRun_settings = simRun.settings
    simRun_settings.starting_rack = 1
    time.sleep(2)
    simRun.compile()
    time.sleep(2)
    simRun.run()
    simRun.update_plots()
    time.sleep(120)

    ## Clear Relay
    print("\n\n**********Clearing Relays**********\n")
    Clear_Relay(t401l_l_ip,23, password_level1='OTTER', password_level2='TAIL')
    Clear_Relay(t401l_r_ip,23, password_level1='OTTER', password_level2='TAIL')
    time.sleep(60)
```

```
Fault_Locations_Loc25 = ["Fault at 0.25 from Local Bus "]
Fault_Locations_Rem25 = ["Fault at 0.75 from Remote Bus"]
Fault_Locations_Loc50 = ["Fault at 0.5 from Local Bus "]
Fault_Locations_Rem50 = ["Fault at 0.5 from Remote Bus"]
Fault_Locations_Loc75 = ["Fault at 0.75 from Local Bus "]
Fault_Locations_Rem75 = ["Fault at 0.25 from Remote Bus"]


case_num = 0
# Changing Load Flow
for l in range (len(load_flow_angle)):
    la = load_flow_angle[l]
    lf_rtds_sharc_sld_SRC_id2 = simRun.get_object(2)
    lf_rtds_sharc_sld_SRC_id2.set_parameter("Ph", str(la))
    time.sleep(2)
    Fault_Locations_Loc25.append(str(load_flow_angle[l]))
    Fault_Locations_Rem25.append(str(load_flow_angle[l]))
    Fault_Locations_Loc50.append(str(load_flow_angle[l]))
    Fault_Locations_Rem50.append(str(load_flow_angle[l]))
    Fault_Locations_Loc75.append(str(load_flow_angle[l]))
    Fault_Locations_Rem75.append(str(load_flow_angle[l]))

    # Changing Fault Resistances
    for r in range (len(fault_resistances)):
        fr = fault_resistances[r]

        Fault_Locations_Loc25.append(str(fault_resistances[r]))
        Fault_Locations_Rem25.append(str(fault_resistances[r]))
        Fault_Locations_Loc50.append(str(fault_resistances[r]))
        Fault_Locations_Rem50.append(str(fault_resistances[r]))
        Fault_Locations_Loc75.append(str(fault_resistances[r]))
        Fault_Locations_Rem75.append(str(fault_resistances[r]))

        for n in range (len(fault_objects_pg)):
            simRun.get_object(fault_objects_pg[n]).set_parameter("AgRon", str(fr))
            simRun.get_object(fault_objects_pg[n]).set_parameter("BgRon", str(fr))
            simRun.get_object(fault_objects_pg[n]).set_parameter("CgRon", str(fr))
        for n in range (len(fault_objects_pp)):
            simRun.get_object(fault_objects_pp[n]).set_parameter("ABRon", str(fr))
```

```
            simRun.get_object(fault_objects_pp[n]).set_parameter("BCRon", str(fr))
            simRun.get_object(fault_objects_pp[n]).set_parameter("CARon", str(fr))

        if case_num > 0:
            simRun.stop()
            time.sleep(120)
            simRun.run()

        for p in range (len(POW_val)):
            simRun.get_object(2372).value = POW_val[p]

            Fault_Locations_Loc25.append(str(POW_val[p]))
            Fault_Locations_Rem25.append(str(POW_val[p]))
            Fault_Locations_Loc50.append(str(POW_val[p]))
            Fault_Locations_Rem50.append(str(POW_val[p]))
            Fault_Locations_Loc75.append(str(POW_val[p]))
            Fault_Locations_Rem75.append(str(POW_val[p]))

            ## Apply Faults
            if flt_25 == 1:
                for f in range (len(fault_triggers_25)):
                    case_num = case_num+1

                    # 25% of Line - Phase-Gnd Faults
                    simRun.get_object(fault_triggers_25[f]).position = 1
                    time.sleep(0.2)
                    simRun.get_object(fault_triggers_25[f]).position = 0

                    case_name = "LF-
Ang="+str(load_flow_angle[l])+"_fltR="+str(fault_resistances[r])+"_fltL=25%_"+"_fl
tT="+str(fault_types[f])+"_POW="+str(POW_val[p])
                    case_dir_loc25 = os.path.join(results_Local,case_name+"\\")
                    case_dir_rem25 = os.path.join(results_Remote,case_name+"\\")
                    os.makedirs(case_dir_loc25)
                    os.makedirs(case_dir_rem25)
                    time.sleep(120)

                    print("\n\n**********Collecting Reports from the Local
T401L**********\n")
                    FTPcollect(t401l_1_ip,case_dir_loc25,case_num,col_MHR,HDR_only)
```

```
                print("\n\n**********Collecting Reports from the Remote
T401L**********\n")
                FTPcollect(t4011_r_ip,case_dir_rem25,case_num,col_MHR,HDR_only)
                time.sleep(10)

                ## Data Collection
                comtrade_dir_loc25 =
os.path.join(case_dir_loc25,"comtradeT401LCase_TDR_"+str(case_num)+".HDR")
                [fault_loc_DE_TW, fault_loc_DE_Z] =
HDR_parser(comtrade_dir_loc25)

                print("DE TW Local Fault Location (0.25): "+fault_loc_DE_TW)
                Fault_Locations_Loc25.append(str(fault_loc_DE_TW))
                print("DE Z-based Local Fault Location (0.25): "+fault_loc_DE_Z)
                Fault_Locations_Loc25.append(str(fault_loc_DE_Z))
                time.sleep(60)

                comtrade_dir_Rem25 =
os.path.join(case_dir_rem25,"comtradeT401LCase_TDR_"+str(case_num)+".HDR")
                [fault_rem_DE_TW, fault_rem_DE_Z] =
HDR_parser(comtrade_dir_Rem25)

                print("DE TW Remote Fault Location (0.75): "+fault_rem_DE_TW)
                Fault_Locations_Rem25.append(str(fault_rem_DE_TW))
                print("DE Z-based Remote Fault Location (0.75): "+fault_rem_DE_Z)
                Fault_Locations_Rem25.append(str(fault_rem_DE_Z))
                time.sleep(60)

                ## Clear Relay
                print("\n\n**********Clearing Relays**********\n")
                Clear_Relay(t4011_l_ip,23, password_level1='OTTER',
password_level2='TAIL')
                Clear_Relay(t4011_r_ip,23, password_level1='OTTER',
password_level2='TAIL')
                time.sleep(30)

            if flt_50 == 1:
                for f in range (len(fault_triggers_50)):
                # 50% of Line - Phase-Gnd Faults
                simRun.get_object(fault_triggers_50[f]).position = 1
```

```
                time.sleep(0.2)
                simRun.get_object(fault_triggers_50[f]).position = 0

                case_name = "LF-
Ang="+str(load_flow_angle[l])+"_fltR="+str(fault_resistances[r])+"_fltL=50%_"+"_fl
tT="+str(fault_types[f])+"_POW="+str(POW_val[p])
                case_dir_loc50 = os.path.join(results_Local,case_name+"\\")
                case_dir_rem50 = os.path.join(results_Remote,case_name+"\\")
                os.makedirs(case_dir_loc50)
                os.makedirs(case_dir_rem50)
                time.sleep(90)

                print("\n\n**********Collecting Reports from the Local
T401L**********\n")
                FTPcollect(t401l_l_ip,case_dir_loc50,case_num,col_MHR,HDR_only)
                print("\n\n**********Collecting Reports from the Remote
T401L**********\n")
                FTPcollect(t401l_r_ip,case_dir_rem50,case_num,col_MHR,HDR_only)
                time.sleep(10)

                ## Data Collection
                comtrade_dir_loc50 =
os.path.join(case_dir_loc50,"comtradeT401LCase_TDR_"+str(case_num)+".HDR")
                [fault_loc_DE_TW, fault_loc_DE_Z] =
HDR_parser(comtrade_dir_loc50)

                print("DE TW Local Fault Location (0.5): "+fault_loc_DE_TW)
                Fault_Locations_Loc50.append(str(fault_loc_DE_TW))
                print("DE Z-based Local Fault Location (0.5): "+fault_loc_DE_Z)
                Fault_Locations_Loc50.append(str(fault_loc_DE_Z))
                time.sleep(60)

                comtrade_dir_Rem50 =
os.path.join(case_dir_rem50,"comtradeT401LCase_TDR_"+str(case_num)+".HDR")
                [fault_rem_DE_TW, fault_rem_DE_Z] =
HDR_parser(comtrade_dir_Rem50)

                print("DE TW Remote Fault Location (0.5): "+fault_rem_DE_TW)
                Fault_Locations_Rem50.append(str(fault_rem_DE_TW))
                print("DE Z-based Remote Fault Location (0.5): "+fault_rem_DE_Z)
```

```
                Fault_Locations_Rem50.append(str(fault_rem_DE_Z))
                time.sleep(60)

                ## Clear Relay
                print("\n\n**********Clearing Relays**********\n")
                Clear_Relay(t401l_l_ip,23, password_level1='OTTER',
password_level2='TAIL')
                Clear_Relay(t401l_r_ip,23, password_level1='OTTER',
password_level2='TAIL')
                time.sleep(30)

            if flt_75 == 1:
                for f in range (len(fault_triggers_75)):
                # 75% of Line - Phase-Gnd Faults
                simRun.get_object(fault_triggers_75[f]).position = 1
                time.sleep(0.2)
                simRun.get_object(fault_triggers_75[f]).position = 0

                case_name = "LF-
Ang="+str(load_flow_angle[l])+"_fltR="+str(fault_resistances[r])+"_fltL=75%_"+"_fl
tT="+str(fault_types[f])+"_POW="+str(POW_val[p])
                case_dir_loc75 = os.path.join(results_Local,case_name+"\\")
                case_dir_rem75 = os.path.join(results_Remote,case_name+"\\")
                os.makedirs(case_dir_loc75)
                os.makedirs(case_dir_rem75)
                time.sleep(60)

                print("\n\n**********Collecting Reports from the Local
T401L**********\n")
                FTPcollect(t401l_l_ip,case_dir_loc75,case_num,col_MHR,HDR_only)
                print("\n\n**********Collecting Reports from the Remote
T401L**********\n")
                FTPcollect(t401l_r_ip,case_dir_rem75,case_num,col_MHR,HDR_only)
                time.sleep(10)

                ## Data Collection
                comtrade_dir_loc75 =
os.path.join(case_dir_loc75,"comtradeT401LCase_TDR_"+str(case_num)+".HDR")
                [fault_loc_DE_TW, fault_loc_DE_Z] =
HDR_parser(comtrade_dir_loc75)
```

```
                print("DE TW Local Fault Location (0.75): "+fault_loc_DE_TW)
                Fault_Locations_Loc75.append(str(fault_loc_DE_TW))
                print("DE Z-based Local Fault Location (0.75): "+fault_loc_DE_Z)
                Fault_Locations_Loc75.append(str(fault_loc_DE_Z))
                time.sleep(60)

                comtrade_dir_Rem75 =
os.path.join(case_dir_rem75,"comtradeT401LCase_TDR_"+str(case_num)+".HDR")
                [fault_rem_DE_TW, fault_rem_DE_Z] =
HDR_parser(comtrade_dir_Rem75)

                print("DE TW Remote Fault Location (0.25): "+fault_rem_DE_TW)
                Fault_Locations_Rem75.append(str(fault_rem_DE_TW))
                print("DE Z-based Remote Fault Location (0.25): "+fault_rem_DE_Z)
                Fault_Locations_Rem75.append(str(fault_rem_DE_Z))
                time.sleep(60)



                ## Clear Relay
                print("\n\n**********Clearing Relays**********\n")
                Clear_Relay(t401l_l_ip,23, password_level1='OTTER',
password_level2='TAIL')
                Clear_Relay(t401l_r_ip,23, password_level1='OTTER',
password_level2='TAIL')
                time.sleep(30)

    simRun.stop()

if flt_25 == 1:
    error25L = []
    error25R = []
    for i in range(len(Fault_Locations_Loc25)):
        try:
            error25L.append(str(abs(float(Fault_Locations_Loc25[i])-2.5)/10*100))
            error25R.append(str(abs(float(Fault_Locations_Rem25[i])-7.5)/10*100))
        except:
            error25L.append("NaN")
            error25R.append("NaN")
```

```
    data25 =
[headers_csv,Fault_Locations_Loc25,Fault_Locations_Rem25,error25L,error25R]
    with open("Results25.csv", "w", newline="") as file:
        writer = csv.writer(file)
        writer.writerows(data25)    # Writes each inner list as a row

if flt_50 == 1:
    error50L = []
    error50R = []
    for i in range(len(Fault_Locations_Loc50)):
        try:
            error50L.append(str(abs(float(Fault_Locations_Loc50[i])-5)/10*100))
            error50R.append(str(abs(float(Fault_Locations_Rem50[i])-5)/10*100))
        except:
            error50L.append("NaN")
            error50R.append("NaN")
    data50 =
[headers_csv,Fault_Locations_Loc50,Fault_Locations_Rem50,error50L,error50R]
    with open("Results50.csv", "w", newline="") as file:
        writer = csv.writer(file)
        writer.writerows(data50)    # Writes each inner list as a row

if flt_75 == 1:
    error75L = []
    error75R = []
    for i in range(len(Fault_Locations_Loc75)):
        try:
            error75L.append(str(abs(float(Fault_Locations_Loc75[i])-7.5)/10*100))
            error75R.append(str(abs(float(Fault_Locations_Rem75[i])-2.5)/10*100))
        except:
            error75L.append("NaN")
            error75R.append("NaN")
    data75 =
[headers_csv,Fault_Locations_Loc75,Fault_Locations_Rem75,error75L,error75R]
    with open("Results75.csv", "w", newline="") as file:
        writer = csv.writer(file)
        writer.writerows(data75)    # Writes each inner list as a row

now = datetime.now()
end_time = now.strftime("%H:%M:%S")
```

```
print("Start Time =", start_time)
print("End Time =", end_time)
```

Figure C.4 Automated Script

APPENDIX D: T401L SETTINGS

The main list of settings configured on the relay for all test cases are defined below. All settings which have a constant value will include their values. If the value is subject to change based on the configuration of the cable, the setting is bolded and an example for transposed and cross-bonded cables are included.

- NFREQ: 60 (System Nominal Frequency)
- PHROT: ABC (Phase Rotation)
- LINEI: IW (The CT(s) Measuring the Line Current)
- CTRW: 400 (CT-W Ratio)
- CTRX: 400 (CT-X Ratio)
- PTRY: 2000.00 (PT-Y Ratio)
- VNOMY: 199 (Nominal System Secondary Voltage)
- **Z1MAG**: 0.27 (Cable's Positive-Sequence Impedance Magnitude in Secondary Ohms)
- **Z1ANG**: 73.42 (Cable's Positive-Sequence Impedance Angle in degrees)
- **Z0MAG**: 0.44 (Cable's Zero-Sequence Impedance Magnitude in Secondary Ohms)
- **Z0ANG**: 38.78 (Cable's Zero-Sequence Impedance Angle in degrees)
- LL: 10.00 (Total Line Length)
- LLUNIT: km (Line Length Units)
- **TWLPT**: 80.24 (Cable TW Propagation Time in microseconds)
- EPORT: Y (Enable Port 6 for Direct Fiber Communication between the two T401Ls)

- TXID: 2 *or* 1(Transmit Identifier for each T401L)
- RXID: 1 *or* 2(Receive Identifier for each T401L)
- FLPORT: P6 (Use Port 6 for fault locating)

APPENDIX E: TWLPT CALCULATIONS

Energization tests are performed to determine the propagation velocity of traveling-waves through a transmission line, in this case a cable. The test is performed with all breakers being open initially. Then the breaker on the local terminal is closed, from which the events are recorded, while the remote terminal's breaker remains open throughout the test. Once the local breaker is closed, TWs propagate through the cable which will be recorded by the T401L when it generates an event based on the disturbance detected by the relay which would assert the TWDD bit (Traveling-wave disturbance detector).

As shown in the example energization test event in section 4.4.2, the time difference between the first TW wave and its reflection is twice the value of TWLPT. Thus, dividing that time by two and entering it in the TW Line Propagation Time parameter of the Bewley diagram and placing the diagram's first TW and reflection tracers on the peak of the appropriate waves, as shown in the second figure, will result in the fault location being determined to be at the full length of the cable (10 km).